Physics – Uspekhi **59** (6) 513 – 530 (2016)

REVIEWS OF TOPICAL PROBLEMS PACS numbers: 52.30.Cv, 96.60.Hv, 96.60.Q –

Current results on the asymptotics of dynamo models

H P Popova

DOI: 10.3367/UFNe.2016.02.037727

Contents

Abstract. Magnetic field generation and evolution models that are capable of describing a large body of observational material are currently available for different celestial bodies. Despite recent decades of great success in numerical magnetic hydrodynamics and in detailed research into some specific problems, asymptotic methods still have to be used to clarify the magnetic field generation mechanism in dynamo theory. In this review, current asymptotic methods are presented together with the results of their application to the simulation of solar, stellar, and galactic magnetic activities.

Keywords: dynamo theory, Sun, stars, galaxies

1. Introduction

The presence of Earth's magnetic field was first suggested in 1600 in the book *De magnete* [1] by the English doctor and natural philosopher W Gilbert. In this book, he described an experiment with a ball made of magnetic ore and a small iron arrow, related the behavior of the magnetic arrow of a compass with the presence of Earth's magnetic field, and assumed that Earth constitutes a big magnet.

H P Popova Lomonosov Moscow State University, Faculty of Physics, Leninskie gory 1, str. 2, 119991 Moscow, Russian Federation;
Lomonosov Moscow State University,
Skobeltsyn Institute of Nuclear Physics,
Leninskie gory 1, str. 2, 119991 Moscow, Russian Federation
E-mail: popovaelp@mail.ru

Received 15 May 2015, revised 8 February 2016
Uspekhi Fizicheskikh Nauk **186** (6) 577 – 596 (2016)
DOI: 10.3367/UFNr.2016.02.037727
Translated by K A Postnov; edited by A M Semikhatov

The magnetic field of the Sun was discovered by Hayle in 1908 [2], and magnetic fields of other stars were discovered fifty years later by Babcock [3].

The discussion of a magnetic field in our Galaxy started in the middle of the 20th century. The magnetic field in the galactic interstellar medium was studied by Alfvén, Fermi, Ginzburg, Syrovatsky, and other prominent scientists [4–14]. The presence of magnetic fields in nearby galaxies was first assumed in 1958 from observations of stellar light polarization in the Andromeda galaxy (M31) [15]. In 1970, optical observations of the Large and Small Magellanic Clouds [16, 17] suggested the presence of magnetic fields in these galaxies. The first measurements of the magnetic field in the M31 galaxy were reported in [18]. Further results of studies of magnetic fields in galaxies can be found in [19–21].

Space research revealed the presence of magnetic fields in different planets (see, e.g., [22] and the references therein).

In 1919, Larmor [23] first attempted to explain the magnetic fields of Earth and the Sun by suggesting the dynamo concept, according to which the magnetic field of a celestial body is sustained by the hydrodynamic motion of an electrically conducting medium.

However, an issue in the dynamo theory arose in 1934, when Cowling proved the so-called anti-dynamo theorem prohibiting the maintenance of an axially symmetric magnetic field by fluid flows [24]. Most celestial bodies under study were assumed to be axially symmetric. This allowed assuming that their field should also be axially symmetric, and then by the anti-dynamo theorem magnetic field generation by a dynamo should be impossible. Later, it was shown that not all axially symmetric equations describing magnetic field generation have axially symmetric solutions. In the dynamo models that have been developed since the 1950s, axially symmetric equations allow nonaxially symmetric

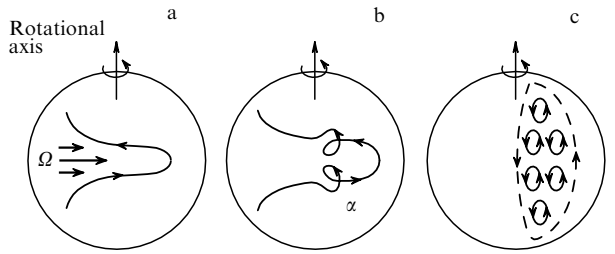

Figure 1. Schematics of the differential rotation Ω and the α-effect.

solutions. The first mathematical models of dynamos were formulated in [25, 26].

In 1955, Parker constructed a dynamo model in which the magnetic field of the Sun was treated as running waves [27]. The magnetic field was represented as the sum of several components: a stronger toroidal (or azimuthal) field elongated along parallels and mainly concentrated toward the solar equator, and a poloidal field elongated along meridians and located in the polar regions. The toroidal magnetic field arises from the poloidal one due to differential rotation inside the convective zone of the Sun. The inverse process of conversion of the toroidal field into poloidal occurs via the so-called α-effect, which occurs due to the mirror symmetry breaking of convection in a rotating body. According to [27], the α-effect arises because the Coriolis force acting on rising and expanding (descending and compressing) eddies leads to the dominance of right eddies in the northern hemisphere (left eddies in the southern hemisphere). The electromotive force, which appears due to Faraday electromagnetic induction, after averaging over velocity pulsations, acquires a component parallel to the mean magnetic field. This force closes the self-excitation chain in a dynamo.

Figure 1 schematically shows the differential rotation Ω and the α-effect. Figure 1a illustrates how differential rotation stretches magnetic field lines along latitudes, Fig. 1b shows how the swirling of magnetic field lines occurs, and Fig. 1c illustrates the emergence of the poloidal field.

Parker suggested (in a heuristic form) averaging the magnetic hydrodynamic (MHD) equations over the mean magnetic field components. In addition, he combined this approach with the effect of an asymmetric rise of magnetic loops, i.e., with asymmetric low-scale motions in the convective zone of the Sun [27, 28].

In 1961, Babcock proposed a dynamo model that was not based on solutions of MHD equations. It only represented a quite broad generalization of solar observations with the use of theoretical approaches known by the beginning of the 1960s [3, 29].

The next important step in formulating dynamo theories of solar cycles was made by Leighton [30]. Unlike Babcock, who had constructed a purely qualitative model, he formulated a semi-quantitative model of the solar activity cycle. Leighton's model is based on the magnetic field amplification by differential rotation. His model is quite similar to Babcock's. According to Babcock's [3, 29] and Leighton's [30] models, the α-effect is assumed to be nonlocal in space and operates near the solar surface. The mechanism of the α-effect in this model is different from the α-effect suggested by Parker. The theory of the α-effect was later developed by Steenbeck, Krause, and Rädler [31].

In 1993, Parker proposed a dynamo model [32] in which the two generation mechanisms for the magnetic field components are spatially separated: the α-effect operates in a turbulent convective layer, and the differential rotation acts closer to the bottom of the convective zone. According to [32], the toroidal field is generated by differential rotation near the convective zone base, the tachocline. Due to magnetic buoyancy, it becomes unstable and rises into the convective zone acting as a filter, which allows the strongest field to rise towards the solar surface to appear as active regions. Weaker fields are captured by convection and are transformed by the α-effect into a poloidal field, which, due to turbulent pumping, plunges into the tachocline region, and the magnetic activity cycle repeats.

The dynamo theory turns out to be applicable to explaining the generation and evolution of the magnetic field not only on the Sun but also on other celestial bodies (stars, planets, and galaxies).

Magnetic fields in the dynamo theory are averaged over a particular space–time scale. This scale is chosen such that all random oscillations of the mechanical velocity of the medium and the electric and magnetic fields are averaged, but at the same time the structure of the spatial distribution of these quantities inside the celestial bodies remain manifest. The propagation of the magnetic field in space is due to turbulent magnetic diffusion. Solutions of such equations can have an oscillating behavior in both space and time. Solar activity cycles provide an example.

In [2, 4–14, 33–82], equations for a magnetic field in a turbulent medium were studied in specific cases. For example, Roberts and Yoshimura formulated first models for large-scale magnetic field generation in planetary and stellar dynamos, Zel'dovich investigated low-scale magnetic fields, and Braginsky constructed models for the generation of Earth's magnetic field.

Research on dynamos became one of those fields of physics that were shaped already in the computer era. Therefore, it clearly demonstrated completely new relations between physics and mathematics. Now it is not necessary to prove that the use of numerical methods extremely broadened the tools of physics. It is much more useful to look at the back side of the problem: attempts to do research based only on computer methods ignoring traditional methods of theoretical physics quite rapidly lead to dead end simply because it is impossible to explore a parameter space even of modest dimensions without understanding the role of individual parameters and their combinations.

This general physical (and also general mathematical) case is especially clear in dynamo studies. Indeed, in the absence of a close physical similarity between dynamo problems and quantum mechanical problems, there is a simple formal analogy between these fields, which enables treating dynamo problems in terms of quantum mechanical problems of specific systems. Because quantum mechanics emerged and developed just before the computer era in physics, it has a number of well-developed analytic methods that help to understand results in quantum chemistry and in other fields based on quantum mechanics. Therefore, it is natural to apply diverse analytic tools of quantum mechanics to dynamo problems. Here, we immediately discover that a comparatively slight change of equations (dynamo equations in the simplest case are of the fourth order, while the Schrödinger equation is of the second order) opens a new world of very different phenomena.

In this review, we present asymptotic methods to study dynamo models developed in recent decades. The methods

and solutions of dynamo problems found by them can be interesting for both the physical and the astrophysical communities.

2. Semiclassical method to study the stellar dynamo

2.1 Semiclassical method to study the 1D linear $\alpha\Omega$ dynamo model

To model the magnetic activity of stars, the $\alpha\Omega$ dynamo mechanism is typically used, which assumes that the α-effect contribution to toroidal magnetic field generation is negligible. We note that the $\alpha\Omega$-dynamo generation regime in the first approximation can be applied to stars, spiral galaxies, and planets.

The magnetic field generation by these dynamo models is verified by the existence of nonvanishing solutions of dynamo equations. To reproduce the solar activity cycle, it is important to show that these models allow reproducing the 11-year cycle of magnetic activity, during which a large-scale magnetic field wave moves from the pole to the equator in each hemisphere. That is, in this case, the problem is to find a nondecaying, oscillating solution of dynamo equations corresponding to a wave moving in the direction found from observations.

Thus, analytic estimates of the simplest dynamo models, which are primarily tailored to find a self-sustaining generation of magnetic field waves analytically and to study their behavior, enable the assessment of the applicability of such models to the description of the magnetic activity of celestial bodies and are used as the basis for more advanced numerical modeling.

Dynamo equations are formally analogous to the Schrödinger equation in quantum mechanics. To solve the Schrödinger equation, various mathematical methods have been developed [83], which can be applied to dynamo equations. Research has shown that the quantum mechanical methods acquire new properties in dynamo theory.

Numerous papers are devoted to the formulation and study of solutions of dynamo equations using an asymptotic method similar to the Wentzel–Kramers–Brillouin (WKB) approximation in quantum mechanics [84]. The use of this method relies on the fact that the solution of mean-field electrodynamic equations can be sought in the form of asymptotic expansions in dimensionless numbers characterizing the intensity of magnetic field generation. In [85], the model of a kinematic dynamo with a high magnetic Reynolds number R_{m} was considered in terms of an artificial flow with exponential partial stretching imitating a stationary random conducting liquid flow. It turned out that in this case, the amplitude of magnetic fields that are periodically dependent only on one coordinate increases exponentially and without bound in time. Each Fourier harmonic of the deviation from this growing field first rapidly increases with increasing the velocity, which is independent of R_{m} in the time interval $t_* \approx t_0 \ln R_{\mathrm{m}}$, and then very rapidly decays. In [86], the approximation of maximum effective generation was used, which is a variant of the semiclassical asymptotic expansion (see, e.g., [84]). It was assumed in [86] that the magnetic field generation source distribution attains a maximum at some point x_0 and that the generated magnetic field is contained within a region near x_0 whose size is determined by the dimensionless dynamo number, and the magnetic field away from x_0 is transported there by diffusion from the maximum generation region. In [87], it was demonstrated that the asymptotic solution in this case correctly reflects the properties of an exact solution of the dynamo equations in nonoscillating or slowly oscillating regimes. However, when the leading eigenfunction of the dynamo problem is a rapidly oscillating solution corresponding to a dynamo wave (magnetic field wave), the maximum effective generation approximation does not reflect the exact features of the solution [88].

A modification of the maximum effective generation approximation is discussed in [82, 89, 90] using the simplest linear one-dimensional $\alpha\Omega$-dynamo model, which gives the correct asymptotic solution in the case of a running dynamo wave. Although these papers were published in 1995 and 1999, the asymptotic analysis was applied to the simplest one-layer Parker dynamo model of 1955, and not the two-layer model of 1993. The authors hoped that, on one hand, such a model would allow taking the main physical principles of the magnetic field evolution into account, and on the other hand, it is quite simple for the construction of a new asymptotic method, which may yield a reasonable result without using more sophisticated mathematical calculations.

The equations of Parker's 1955 $\alpha\Omega$-dynamo model [27] can be formally derived from the complete mean-field electrodynamic equations [31] under the assumption that the dynamo wave propagates in a thin spherical shell (for example, in the inverse layer). In deriving these equations, the magnetic field is averaged over the radius inside some spherical shell where the dynamo operates, and the terms describing curvature effects near the pole are omitted [91]. In this case, the dynamo equations are

$$\frac{\partial A}{\partial t} = \alpha B + \frac{\partial^2 A}{\partial \theta^2}\,, \tag{1}$$

$$\frac{\partial B}{\partial t} = -D\cos\theta\,\frac{\partial A}{\partial \theta} + \frac{\partial^2 B}{\partial \theta^2}\,. \tag{2}$$

Here, B is the toroidal magnetic field, A is proportional to the toroidal component of the vector potential, which determinates the poloidal magnetic field, θ is the latitude measured from the equator, and t is the time measured in units of the diffusion time R^2/β. Distances are measured in units of the convective zone radius R (to be specific, we use the inner radius); β is the turbulent diffusion coefficient. The terms αB and $D\cos\theta\,\partial A/\partial\theta$ describe the respective contributions from the α-effect and differential rotation to the magnetic field generation. The factor $\cos\theta$ accounts for the shortening of the parallel length near the pole. Equations (1) and (2) are written in dimensionless units, with the amplitudes of the α-effect, the angular velocity gradient, and the turbulent diffusion coefficient combined in one dimensionless dynamo number D. This model is an $\alpha\Omega$-approximation. In diffusion terms, curvature effects are omitted and it is assumed for simplicity that the radial gradient of the angular velocity does not change with θ. By the symmetry $\alpha(-\theta) = -\alpha(\theta)$, Eqns (1) and (2) can be applied only for one (northern) hemisphere, with the antisymmetry (dipole symmetry) or symmetry (quadrupole symmetry) conditions imposed on the equator. Because the solar magnetic field has the dipole symmetry, only the dipole symmetry is considered in papers devoted to magnetic field generation.

Figure 2a, b shows the schematics of the solar magnetic field structure with dipole and quadrupole symmetry. The

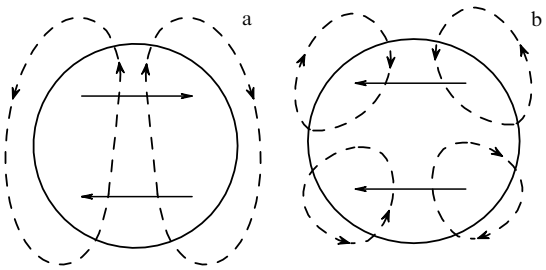

Figure 2. Structure of the solar magnetic field with (a) dipole and (b) quadrupole symmetry. The poloidal and toroidal fields are respectively shown by the dashed and solid lines.

poloidal and toroidal field components are shown by the dashed and solid lines.

As shown in [82], the solution of Eqns (1) and (2) can be sought in the form of the expansion in a power series in the dynamo number D:

$$\begin{pmatrix} \hat{A} \\ \hat{B} \end{pmatrix} = \exp\left(\mathrm{i}|D|^{1/3}S + \gamma t\right)\left(f_0 + |D|^{-1/3}f_1 + \ldots\right), \qquad (3)$$

where

$$\gamma = |D|^{2/3}\Gamma + |D|^{1/3}\Gamma_1 + \ldots, \qquad (4)$$

$$f_0 = \begin{pmatrix} \mu \\ \nu \end{pmatrix}, \quad f_1 = \begin{pmatrix} \mu_1 \\ \nu_1 \end{pmatrix}, \ldots . \qquad (5)$$

Here, S, μ, ν, μ_1, and ν_1 are smooth functions and $|D| \gg 1$; S is analogous to the action in quantum mechanics, and its derivative $k = S'$ corresponds to the momentum, or wave vector, which is complex in this case. The complex γ determines an eigenvalue, and its real and imaginary parts respectively give the rate of growth and the duration of the activity cycle. The factors $|D|^{2/3}$ in the imaginary growth rate and $|D|^{1/3}$ in the action are chosen such that the differential rotation, the α-effect, the eigenvalue, and the dissipation are of the same order to enter the leading term of the expansion. Expression (3) is an analog of the wave function in quantum mechanics. We note that in this model, the α-effect corresponds to the potential in quantum mechanics and γ corresponds to energy levels.

Substituting the chosen form of the sought solution in Parker's equations and equating coefficients at the terms with the same powers of $|D|$ yields a homogeneous system of equations, linear in the leading order, for the functions S, μ, ν, and the constant Γ. The solvability condition of this system gives the dispersion relation for the dynamo wave frequency and its wave vector, i.e., the Hamilton–Jacobi equation

$$[\Gamma + k^2]^2 - \mathrm{i}\hat{\alpha}k = 0\,, \qquad (6)$$

where $\hat{\alpha} = \alpha\cos\theta$.

The main problem in constructing the asymptotic solution of dynamo equations is in studying Eqn (6). Equation (6) is a fourth-order equation in $k(\alpha)$ and has four different complex solutions at a given $\hat{\alpha}$.

Figure 3 shows the roots k of Eqn (6) on the complex plane as functions of the parameter θ. The turning points (at which the end of one branch of the solution coincides with the end of another branch) are shown by circles. The corresponding values of θ are shown in parentheses. Each branch is

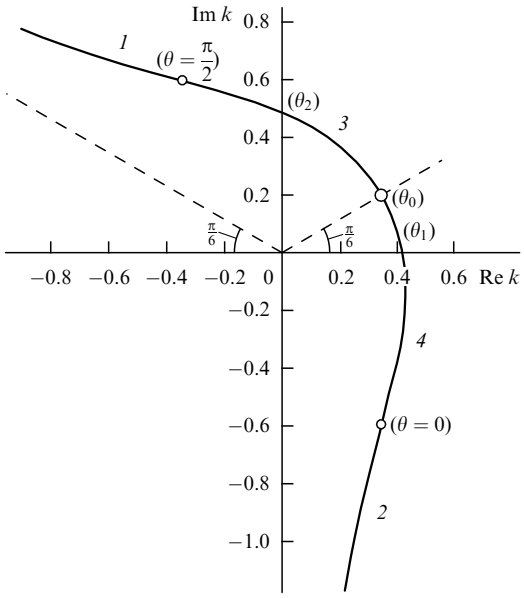

Figure 3. Four branches of the momentum k on the complex plane for a given value of Γ_0 [82].

numbered. It is shown in [82] that two branches (*3* and *4* in Fig. 3) of Eqn (6), which match smoothly, correspond to a wave propagating from the pole toward the equator.

The behavior of dynamo waves in the framework of the simplest generalizations of the $\alpha\Omega$-dynamo model was studied in detail in [90] (near the poles) and [92] (near the equator). It was shown in [90] that incident and reflected waves appear near the poles, and an exact solution of the $\alpha\Omega$-dynamo equations near the poles was obtained. The amplitude of the reflected wave was also found to be smaller than that of the incident wave. The existence of a wave incident on the pole was also confirmed by observations [93].

According to [90], to construct the solution near the poles, it is necessary to match branches *3* and *1* (see Fig. 3), i.e., the point Γ_1 at which the branches are matched must be found. To do this, a higher-order asymptotic expansion than that given in [94–96] should be constructed. In [90], an expression for Γ_1 was obtained, which is an analog of the Bohr–Sommerfeld quantization condition in quantum mechanics.

It was shown in [82] that the maximum of the obtained solution is not at the turning point θ_0 where generation sources are maximal, but at the point θ_1 whose location for any function $\hat{\alpha}$ is determined by the condition $\hat{\alpha}_1 = \hat{\alpha}(\theta_1)/\hat{\alpha}_* \approx 0.8052$, where $\hat{\alpha}_*$ is the maximum value of the function $\hat{\alpha}$. The point θ_1 is calculated from the following conditions: $\mathrm{Im}\,k = 0$ and $\mathrm{Im}\,S(\theta)$ is minimum. In the simplest case $\alpha = \sin\theta$, θ_1 is equal to 0.468, i.e., approximately 26.8°.

The physical interpretation of this result is that the maximum of the solution is shifted from the maximum generation point along the dynamo wave propagation. The wave amplitude increases most rapidly at the point θ_0, but continues growing with further propagation, and dissipation effects start dominating over generation effects beyond the point θ_1. We note that observations show that solar spots, which are tracers of the dynamo wave of the toroidal field, arise at low latitudes from 0 to 30°. Figure 4 presents the observed latitude–time distribution of solar spots (the so-called butterfly diagram).

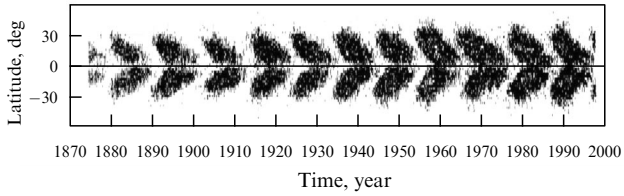

Figure 4. Butterfly diagram of solar spots (http://solarscience. msfc.nasa. gov/images/bfly.gif).

In [82], the dynamo wave was shown to propagate in the main part of the studied domain from the pole to the equator, in accordance with observations. For any function $\alpha(\theta)$, $\mathrm{Re}\, S(\theta)$ changes sign at the point $\theta_2 > \theta_0$ determined by the relation $\hat{\alpha}_2 = \hat{\alpha}(\theta_2)/\hat{\alpha}_* \approx 0.3445$, and for $\theta > \theta_2$ the dynamo wave propagates in the opposite direction. For $\alpha = \sin\theta$, the parameter $\theta_2 = 1.39 \approx 80°$, in agreement with observations [93]. Such a dynamo wave has a much lower amplitude than the dynamo wave propagating toward the equator and decays when approaching the pole. The ratio R of the magnetic field amplitudes at the maximum amplitude point θ_1 and at the point of the propagation direction reversal θ_2 is

$$R = \exp\left(|D|^{1/3} \int_{\theta_1}^{\theta_2} \mathrm{Im}\, k(\theta)\, \mathrm{d}\theta\right). \tag{7}$$

For the solar dynamo number $|D| \sim 10^3 - 10^4$, we obtain $R \approx 7.1 - 68$. This is close to the observed ratio, which is 20–50 [97]. The excitation threshold, i.e., the dynamo number $|D|_{\mathrm{cr}}$ at which the magnetic field generation begins, is $|D|_{\mathrm{cr}} = 40.4$ for $\alpha(\theta) = \sin\theta$. This is much smaller than $|D|_{\mathrm{cr}}$ obtained from numerical calculations; therefore, the excitation threshold should be derived from the applicability conditions of Eqns (1) and (2).

In [92], the dynamo wave behavior near the solar equator was studied in the Parker approximation. To study the behavior of dynamo waves near the equator, the second of the four branches $k(\theta)$ obtained from Eqn (6) is used. The asymptotic analysis revealed that a dynamo wave arising at the middle latitudes of the northern hemisphere does not vanish by reaching the equator but enters the southern hemisphere, where it propagates in the polar direction and rapidly decays. The dynamo wave in the southern hemisphere behaves in a similar way. The angular distance up to which these waves penetrate into the opposite hemispheres can be as high as ten degrees. It can be assumed that this phenomenon was especially clearly observed at the final phase of the Maunder minimum [98, 99]. On the butterfly diagrams of that period, the solar activity cycle appeared as one dynamo wave propagating in the southern hemisphere, and the dynamo wave in the northern hemisphere was suppressed. The butterfly diagrams show how the activity wave slightly extends to the northern hemisphere from the southern. If this phenomenon is due to the effect obtained, the polarity of spots in the northern and southern hemispheres should be the same. However, observations at that time did not report the spot polarity. According to modern observations of the 22-year cycles, it is virtually impossible to find a weak wave penetrating from the southern hemisphere due to the presence of the strong main wave of the northern hemisphere. However, there are activity tracers propagating from the equator to the poles (for example, far ultraviolet lines; see, e.g., [100]), and active regions violating the Hale polarity rule are also known [101]. Possibly, these phenomena can be related to the effect of dynamo wave penetration from one hemisphere to another. It was shown in [92] that the dipole magnetic configuration grows more rapidly than the quadrupole one, and the complex growth rates of these configurations are close to each other. The authors of [92] assume that this may indicate the possibility of the long-term existence of a nondipole configuration, if it was somehow formed. The authors of [92] relate this effect to the long-term existence of a mixed-parity configuration at the end of the Maunder minimum, although its appearance remains obscure.

2.2 Semiclassical method to study the 1D nonlinear $\alpha\Omega$-dynamo model

To explore more realistic models of magnetic field generation, it is worth passing from linear to nonlinear models. In [102–104], $\alpha\Omega$-dynamo equations with a nonlinear α-effect are studied under the assumption that the thickness of the convective shell is small compared to its radius.

The simplest nonlinear dynamo problem, whose periodic solutions were investigated in [102–104], has the form

$$\frac{\partial A}{\partial t} = \alpha(B)B + \frac{\partial^2 A}{\partial \theta^2} - \lambda^{-2}\mu^2 A\,, \tag{8}$$

$$\frac{\partial B}{\partial t} = D\,\frac{\partial A}{\partial \theta} + \frac{\partial^2 B}{\partial \theta^2} - \lambda^{-2}\mu^2 B\,. \tag{9}$$

Here, B is the toroidal magnetic field, A is the vector potential, θ is the latitude measured from the pole, t is time, $D = R_\alpha R_\omega \bar{G} \sin\bar{\theta}$, where $\bar{\theta}$ is the latitude at which the dynamo wave is located, and R_α and R_ω are amplitudes of the α-effect and differential rotation. The normalization is the same as in Eqns (1) and (2). The function $\bar{G} = G(\bar{\theta})$ is defined as a measure of the angular rotation radial gradient. We have a small dimensionless parameter $\lambda = h/R$, where h is the convective zone thickness and R is its inner radius; μ is the radial wave number, with μ^{-1} being the characteristic size of the magnetic field distribution (as well as its potential) in the radial direction. As the characteristic size decreases, the contribution of the radial diffusion of the magnetic field increases and its generation by the dynamo mechanism is hampered. For moderate dynamo numbers typical for the solar dynamo, μ^{-1} is of the order of the convective zone thickness. Thus, this model accounts for the diffusion transport of the magnetic field across the convective zone.

In the problem considered, the toroidal magnetic field component B is much larger than the poloidal one, and therefore the α-effect can be considered to be dependent on the toroidal magnetic field component only. Two forms of the nonlinearity were considered in [102–104]:

$$\alpha(B) = \alpha_0\left(1 - \frac{B^2}{B_0^2}\right), \tag{10}$$

$$\alpha(B) = \frac{\alpha_0}{1 + B^2/B_0^2}\,. \tag{11}$$

Here, B_0 determines the magnetic field amplitude at which nonlinear effects becomes essential. In dimensionless form, we set $\alpha_0 = \alpha_* = 1$.

Periodic solutions of Eqns (8) and (9) can be found in the kinematic approximation, with α assumed to be independent of B. In this case, the solution has the form of a harmonic

dynamo wave,

$$A = |D|^{-2/3} a(\xi) B_0 \,, \qquad B = b(\xi) B_0 \,, \tag{12}$$

where $a = a_* \exp(\mathrm{i}\xi)$ and $b = b_* \exp(\mathrm{i}\xi)$ are dimensionless functions, B_0 is the magnetic field unit that in the kinematic approximation can be chosen in an arbitrary form, and

$$\xi = (\omega - \mathrm{i}\gamma) t + k\theta \,, \tag{13}$$

where ω, γ, and k are real constants.

Substituting (12) and (13) in (8) and (9) yields

$$\gamma = |D|^{2/3} \Gamma \,, \quad \omega = |D|^{2/3} \Omega \,, \quad k = |D|^{2/3} K \,. \tag{14}$$

The first three terms in each of Eqns (8) and (9) are now of the same order. The last term in these equations has the same order if

$$D^{1/3} \lambda \sim 1 \,. \tag{15}$$

If $D^{1/3}\lambda \gg 1$, the last term in Eqns (8) and (9) can be discarded and Eqns (8) and (9) are transformed into Eqns (1) and (2). When $D^{1/3}\lambda \ll 1$, generation of dynamo waves in Eqns (8) and (9) is impossible because the dynamo number becomes smaller than the critical value. Therefore, it is sufficient to consider the case in (15). We assume that $D = \lambda^{-3}$, because μ can always be renormalized appropriately. By substituting (15) and $D = \lambda^{-3}$ in (8) and (9), we obtain that the growth rate Γ is decreased compared with Parker's dynamo case in Section 2.1 by μ^2. Solving the eigenvector and eigenvalue problem, we obtain

$$\Gamma = \sqrt{\frac{|K|}{2}} - K^2 - \mu^2 \,, \quad |K| = 2\Omega^2 \,, \quad \frac{a_*}{b_*} = \frac{1}{\Omega(\mathrm{i} - 1)} \,. \tag{16}$$

In this approximation, the dynamo wave has the same asymptotic properties as the one in dynamo model (1) and (2), except that the curve $\Gamma(K)$ is shifted by μ^2 toward negative values of Γ. The maximum growth rate for problem (8), (9) is $\Gamma_{\max} = (3/8)(1/2)^{1/3} - \mu^2$.

This result implies that only waves with certain wavelengths can form in the convective shell. For each μ, there are lower and upper wavelengths. In the case of algebraic suppression of helicity, asymptotic properties of dynamo waves in a stationary nonlinear regime were considered in [103] with relations (12) and (14) assumed to hold and with $D = \lambda^{-3}$. The magnetic field unit B_0 is then not arbitrary but is determined by the equipartition condition. The solution is assumed to be periodic, with the period in the range $0 < \xi \leqslant 2\pi$. Nonlinear equations in this case take the form

$$\Omega \frac{\partial a}{\partial \xi} = \alpha(b) b + K^2 \frac{\partial^2 a}{\partial \xi^2} - \mu^2 a \,, \tag{17}$$

$$\Omega \frac{\partial b}{\partial \xi} = -K \frac{\partial a}{\partial \xi} + K^2 \frac{\partial^2 b}{\partial \xi^2} - \mu^2 a \,. \tag{18}$$

As shown in [103], the solution of the problem can be sought in the form $a(\xi) = a_1 \sin\xi + a_2 \cos\xi$, $b(\xi) = b_1 \sin\xi$. In [103], magnetic field generation was found to occur almost identically for both nonlinearities (10) and (11). The dynamo wave amplitude is finite, with a maximum at some value of K that increases with μ. The maximum value decreases with μ. At μ exceeding some maximal value $\mu_{\max} \approx 0.55$, no generation occurs. In the approximation considered, only dynamo waves with a zero mean can be generated. We note that in model (1), (2), waves with both zero and nonzero mean values can exist. This result implies the possibility of mixed-parity wave generation, which violates the equatorial asymmetry in the solar cycle. In model (1), (2), waves with an arbitrarily small wave number K can exist, and nonlinear model (8), (9) has a lower bound on the wavelength, and waves with the wave number below some critical value cannot exist. This is a manifestation of the finite thickness of the convective shell.

In [102], system of equations (8), (9) with algebraic suppression of helicity is studied for the dynamo number $D(\theta)$ depending on the latitude θ. It is also shown in [102] that the dynamo wave is bounded within a latitude interval $\theta_1 < \theta < \theta_2$. It is destroyed with finite amplitude at the high latitude θ_2, where D reaches some threshold value D_{T} that fixes the dynamo wave frequency at a constant μ. At lower latitudes $\theta < \theta_2$, the magnetic field amplitude depends on $D(\theta)$, which, unlike μ, can change on a time scale much longer than the cycle period. The wave amplitude decreases with decreasing latitude and vanishes at a low latitude θ_1 where D becomes smaller than the threshold value $D_{\mathrm{P}} < D_{\mathrm{T}}$ and can generate only linear waves. The model has two important features. First, the dynamo wave amplitude depends on the dynamo number, while the frequency is virtually independent of it. Thus, differences in the amplitude of the 11-year solar activity cycles can be related to fluctuations of the α-effect or differential rotation, on which the dynamo number depends. Second, the dynamo wave is fully nonlinear, because $D_{\mathrm{T}} - D_{\mathrm{P}} = O(D_{\mathrm{P}})$. It has been shown that the dynamo wave is stable unless it has a small amplitude at low latitudes close to θ_1. Numerical calculations confirmed the analytic results.

2.3 Semiclassical method to study the 2D linear $\alpha\Omega$-dynamo model

In [105], the two-dimensional problem of the linear $\alpha\Omega$-dynamo is studied using a method similar to the WKB approximation. In this case, the system of equations for the generation of an axially symmetric magnetic field in a differentially rotating spherical layer has the form

$$\frac{\partial A}{\partial t} = \alpha B + \beta \frac{1}{r^2} \frac{\partial}{\partial \theta} \left(\frac{1}{\cos\theta} \frac{\partial (A \cos\theta)}{\partial \theta} \right) + \beta \frac{1}{r} \frac{\partial^2 (rA)}{\partial r^2} \,, \tag{19}$$

$$\frac{\partial B}{\partial t} = \beta \frac{1}{r^2} \frac{\partial}{\partial \theta} \left(\frac{1}{\cos\theta} \frac{\partial (B \cos\theta)}{\partial \theta} \right) + \beta \frac{1}{r} \frac{\partial^2 (rB)}{\partial r^2} + \frac{D}{r} \frac{\partial \Omega}{\partial \theta} \frac{\partial (rA \cos\theta)}{\partial r} - \frac{D}{r} \frac{\partial \Omega}{\partial r} \frac{\partial (rA \cos\theta)}{\partial \theta} \,, \tag{20}$$

where we use the same notation as in (1) and (2). The field, the angular velocity Ω, and the α-effect depend on the radius r and the latitude θ in a spherical coordinate system centered on the Sun (a star). The value $\theta = 0$ corresponds to the equator. As in problem (1), (2), it is assumed that the contribution of the α-effect to the toroidal magnetic field generation can be ignored.

The solution of Eqns (19) and (20) can be sought in the wave form. In this case, it can be written in a form similar to (3):

$$\begin{pmatrix} \hat{A}(r,\theta) \\ \hat{B}(r,\theta) \end{pmatrix} = \begin{pmatrix} A(r,\theta) \\ |D|^{2/3} B(r,\theta) \end{pmatrix} = \begin{pmatrix} \mu(r,\theta) \\ \nu(r,\theta) \end{pmatrix} \exp\left(|D|^{2/3} \Gamma t + \mathrm{i} |D|^{1/3} S(r,\theta) \right) . \tag{21}$$

Substituting the chosen solution in Eqns (19) and (20), we obtain an algebraic system of equations for μ and ν. The solvability condition for this system yields the dispersion relation for the dynamo wave frequency and wave vector, i.e., the Hamilton–Jacobi equation:

$$\left[\Gamma + (S_r)^2 + \frac{1}{r^2}(S_\theta)^2\right]^2 = \mathrm{i}r\alpha\cos\theta\,(GS_\theta + FS_r)\,. \qquad (22)$$

Here, $G = (1/r)\,\partial\Omega/\partial r$, $F = -(1/r)\,\partial\Omega/\partial\theta$, Γ is the eigenvalue of the leading mode, and S_r and S_θ are partial derivatives of S.

The solution of Eqn (22) should correspond to a smooth solution of Eqns (19) and (20) decaying at infinity, i.e., far away from the generation region. To study the problem, the stationary point for (22) must be found [106]. A method for finding solutions satisfying these conditions was proposed in [107, 108].

To seek the stationary point, it is necessary to replace Γ with a new function $\gamma(r, \theta, S_r, S_\theta)$. A constant Γ exists only for a bounded set of arguments (r, θ) and functions S. The function γ is defined on the set (r, θ, S_r, S_θ), which can be treated as its arguments. For the set of arguments (r_0, θ_0, S_{r0}, $S_{\theta 0}$), the following equations hold:

$$\frac{\partial\gamma}{\partial r} = 0\,, \quad \frac{\partial\gamma}{\partial\theta} = 0\,, \quad \frac{\partial\gamma}{\partial S_r} = 0\,, \quad \frac{\partial\gamma}{\partial S_\theta} = 0\,. \qquad (23)$$

A solution of Eqns (23) determines the sought eigenvalues and eigenfunctions of Eqn (22) as follows:

$$\begin{aligned} &\Gamma = \gamma(r_0, \theta_0, S_{r0}, S_{\theta 0})\,, \\ &S_r(r_0, \theta_0) = S_{r0}\,, \quad \theta(S_{r0}, \theta_0) = S_{\theta 0}\,. \end{aligned} \qquad (24)$$

It was shown in [105] that the asymptotic solutions based on this approximation provide a sufficiently correct explanation of the existing solar observations. They also agree with results of numerical analysis. The main feature of the solution obtained in the two-dimensional model is its correspondence to the Yoshimura law, according to which the dynamo wave propagates along a line of constant angular velocity.

In [105], for large dynamo numbers, a solution was constructed based on a realistic description of the internal rotation derived from helioseismological data. The analysis revealed two centers of dynamo wave generation: at low and high latitudes. Waves generated at low and high latitudes respectively propagate toward the equator and toward the pole. This result is in agreement with conclusions in [109]. Maxima of both waves are shifted in the propagation direction. The relative value of the high-latitude generation sources is about three times as high as that of low-latitude ones. The location of the maximum of the generation source of the wave propagating toward the equator lies behind the convection zone at the point ($r = 0.66$, $\theta = 12°$). The maximum of the wave propagating toward the pole is at the point ($r = 0.68$, $\theta = 68°$). As shown in [105], the obtained asymptotic solution is qualitatively, and to a great extent quantitatively, the same for different admissible α-effect profiles.

In [110–112], similar dynamo models were studied using asymptotic WKB methods by assuming that the maxima of the solutions correspond to those of the generation sources (using the maximum effective generation method). The authors used only the first two conditions in (23). In [110], the main properties of generated magnetic field waves were studied in the case of arbitrary angular rotation velocities. Dynamo waves were found to propagate along constant rotation surfaces and their amplitude maxima turned out to be shifted in the propagation direction from the intensity maxima of generation sources. As in [105], two dynamic waves propagating from the middle latitudes toward the poles were obtained. With an increasing magnetic field in one of the waves, the amplitude of the magnetic field in the other wave decreases. Those latitudes where the maximum and the point of wave divergence toward the poles and the equator are located depend on the relation between the radial and latitudinal gradients of the rotation angular velocity.

2.4 Semiclassical method to study the linear $\alpha\Omega$ dynamo with meridian flows in one- and two-layer media

Many observations show that large-scale motions are present in the solar convective zone. In [113], the meridional circulation velocity was estimated and the latitudinal profile of the flow and its time variability during the solar cycle were obtained. Based on Doppler measurements [114], matter on the convective zone surface was found to flow toward the poles. Helioseismological data [115] revealed a flow toward the poles up to depths of about 12,000 km and a quite slow convergent flow toward latitudes where solar spots are most frequently formed. The analysis of the motion of solar spots in [116–123] showed that matter flows away from latitudes with the maximum solar spot activity. Meridional flows were also studied using shifts of solar spots [118–123]. Tuominen showed that spots at latitudes below 16° move toward the equator, and spots at higher latitudes move toward the poles, with a velocity increasing with the latitude. In [124, 125], it was shown how the latitudinal inhomogeneity of tracers affects the determination of the resulting meridional flow.

The key role of meridional flows in large-scale solar spot dynamics was established in [126]. According to [70, 72, 127], the motion of the spot formation region toward the equator, which is observed on the Sun, is explained by the transport of the toroidal magnetic field by meridional flows deep inside the Sun. The motion of the poloidal field toward the poles, according to [128–130], can be due to the meridional flow on the solar surface. It was assumed in [131, 132] that the meridional circulation is one of the factors responsible for the formation of differential rotation in the Sun and stars.

Studies of Parker's dynamo model for a one-layer medium [94–96] showed that the meridional flows of matter directed oppositely to the dynamo wave propagation can significantly increase the activity cycle duration.

Parker's equations for a one-layer medium with the meridional circulation taken into account have the form

$$\frac{\partial A}{\partial t} + V\frac{\partial A}{\partial\theta} = \alpha B + \frac{\partial^2 A}{\partial\theta^2}\,, \qquad (25)$$

$$\frac{\partial B}{\partial t} + \frac{\partial(VB)}{\partial\theta} = -D\cos\theta\,\frac{\partial A}{\partial\theta} + \frac{\partial^2 B}{\partial\theta^2}\,. \qquad (26)$$

The notation here is the same as in Eqns (1) and (2); V is the meridional circulation that can depend on the latitude. Solutions of system (25), (26) can be sought in a form similar to (3):

$$\begin{pmatrix}\hat{A}\\ \hat{B}\end{pmatrix} = \begin{pmatrix}A\\ |D|^{2/3}B\end{pmatrix} = \begin{pmatrix}\mu\\ \nu\end{pmatrix}\exp\left(|D|^{2/3}\gamma t + \mathrm{i}|D|^{1/3}S\right). \qquad (27)$$

We assume that the meridional circulation enters the leading term of the asymptotic expansion. Then

$$V = |D|^{1/3} v(\theta)\,. \tag{28}$$

Substituting the chosen form of the sought solution in Parker's equations, we obtain an algebraic system of equations for μ and v. The solvability condition for this system yields the dispersion relation for the dynamo wave frequency and its wave vector, i.e., the Hamilton–Jacobi equation

$$[\Gamma + \mathrm{i}kv + k^2]^2 - \mathrm{i}\hat{\alpha}k = 0\,, \tag{29}$$

where $\hat{\alpha} = \alpha\cos\theta$.

To solve Eqns (25) and (26) and to study the behavior of the dynamo wave for different forms of the meridional circulation, Eqn (29) was investigated in [96] using a method similar to that used in [82], which is described in Section 2.1.

The cases where $v = \text{const}$, $v = \tilde{v}\sin(2\theta)$, and $v = \tilde{v}/\sin(2\theta)$ were considered in [96]. It was shown that there is a range of meridional circulation within the observed range (about several meters per second) at which the solar cycle duration obtained in model (25), (26) nearly matches observations. Above some value of the meridional circulation, the dynamo waves transform into steadily growing magnetic field configurations. The meridional circulation does not reverse the dynamo wave propagation direction. The dynamo wave configuration is strongly affected by the latitudinal dependence of the matter velocity, which opens up the fundamental possibility of reconstructing the meridional circulation profile from solar activity measurements.

The results obtained for problem (25), (26) in [94–96] were confirmed in [133] using Airy functions. The asymptotic solution for the regime in which the magnetic field steadily grows was studied in [133] in greater detail.

An analysis of a one-layer medium describes one-sided matter flow and does not allow a description of its reversal. For a more adequate treatment, a two-layer medium with oppositely directed meridional motions and different diffusion coefficients was considered in [134]. The two-layer model enables taking some effects of the 2D model into account without complicating the asymptotic behavior arising in the 2D problem.

In the case of a two-layer medium, it is possible to introduce the meridional circulation into Parker's equations [32], in analogy with the one-layer problem. Then

$$\frac{\partial B}{\partial t} + \frac{\partial (VB)}{\partial \theta} = \beta\Delta B\,, \qquad \frac{\partial A}{\partial t} + V\frac{\partial A}{\partial \theta} = \alpha B + \beta\Delta A\,, \tag{30}$$

$$\frac{\partial b}{\partial t} + \frac{\partial (vb)}{\partial \theta} = D\cos\theta\,\frac{\partial a}{\partial \theta} + \Delta b\,, \qquad \frac{\partial a}{\partial t} + v\frac{\partial a}{\partial \theta} = \Delta a\,, \tag{31}$$

where B, A, and $V(\theta)$ stand for the magnetic field, magnetic potential, and meridional circulation on the first layer where the α-effect operates, b, a, and $v(\theta)$ are the same quantities in the second layer, where the differential rotation dominates, D is the dynamo number, and β is the ratio of the turbulent diffusion coefficients in the first and second layers. The boundary conditions have the form

$$b = B\,, \qquad a = A\,, \qquad \frac{\partial b}{\partial r} = \beta\,\frac{\partial B}{\partial r}\,, \qquad \frac{\partial a}{\partial r} = \frac{\partial A}{\partial r}\,. \tag{32}$$

Equations (30) and (31) do not take the curvature effect into account and hence do not allow deciding which of the layers is external or internal. However, taking observational data into account [114, 115, 118], it is possible to assume that matter in the external layer moves from the equator to the poles, i.e., against the dynamo wave propagation; in the polar regions, it transits to the internal layer and moves there from the poles toward the equator and transits to the external layer in the equatorial region. Therefore, if the positive meridional circulation is concentrated in one of the layers, it can be considered to be the external one. Similarly, if the meridional circulation has a negative sign in the layer, it can be considered to be the internal one. We stress that the circulation in each layer has the opposite sign.

Model (30), (31) assumes that the magnetic field has the dipole symmetry and the dynamo wave propagates from the poles to the equator in both layers. The thickness and density in the layers can be different. A solution of the system of equations (30), (31) can be represented in the form

$$B = \mu\exp\left(\mathrm{i}D^{1/3}S\theta + \gamma D^{2/3}t - \mathrm{i}D^{1/3}m_1 r\right), \tag{33}$$

$$A = (v + v_1 r)\exp\left(\mathrm{i}D^{1/3}S\theta + \gamma D^{2/3}t - \mathrm{i}D^{1/3}m_1 r\right), \tag{34}$$

$$a = \zeta\exp\left(\mathrm{i}D^{1/3}S\theta + \gamma D^{2/3}t + \mathrm{i}D^{1/3}m_2 r\right), \tag{35}$$

$$b = (\chi + \chi_1 r)\exp\left(\mathrm{i}D^{1/3}S\theta + \gamma D^{2/3}t - \mathrm{i}D^{1/3}m_2 r\right), \tag{36}$$

where γ, v, v_1, ζ, χ, χ_1, m_1, and m_2 are arbitrary constants and $S = \int k\,\mathrm{d}\theta$.

The Hamilton–Jacobi equation with meridional circulation has the form

$$\left(\beta\sqrt{-\frac{\gamma + \mathrm{i}Vk}{\beta} - k^2} + \sqrt{-\gamma - \mathrm{i}vk - k^2}\right) \times \left(\sqrt{-\frac{\gamma + \mathrm{i}Vk}{\beta} - k^2} + \sqrt{-\gamma - \mathrm{i}vk - k^2}\right) = -\frac{4\hat{\alpha}k}{\mathrm{i}\beta\sqrt{-\gamma - \mathrm{i}vk - k^2}\,\sqrt{-(\gamma + \mathrm{i}Vk)/\beta - k^2}}\,. \tag{37}$$

Equation (37) was studied in [134], with the conclusion that the intensive meridional circulation in the layers can slow the dynamo wave propagation.

Figure 5 illustrates the ratio of the meridional circulation amplitudes $V(\theta)$ and $v(\theta)$ in the layers and the ratio of the turbulent diffusion coefficients β at which the model gives the 22-year solar cycle. The quantity $V(\theta)$ corresponds to the meridional circulation of the layer dominated by the α-effect, and $v(\theta)$ corresponds to the layer dominated by the differential rotation effect. The values of the meridional circulation are given for the dynamo numbers ranging from -10^3 to -10^4. The levels are marked with values of β. For the cycle duration to be 22 years, as follows from this figure, either the meridional circulation has to be enhanced in both layers or β has to be increased. The stronger the meridional motion of matter in the upper layer relative to the inner one, the lower β can be. If the meridional motion of matter in the internal layer is higher than in the external one, to ensure the 22-year cycle β should be higher relative to the previous case.

When the meridional circulation is directed oppositely to the dynamo wave propagation in the layer dominated by differential rotation, and conversely in the layer with the

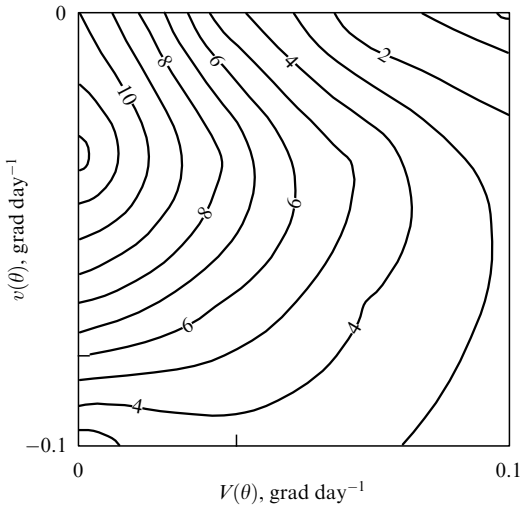

Figure 5. Diagram for β, $V(\theta)$, and $v(\theta)$ at which the model reproduces the 22-year cycle [134].

α-effect, the dependence of β as a function of $V(\theta)$ and $v(\theta)$ is identical. In other words, the dependence of the cycle duration on β is invariant under transposing $V(\theta)$ and $v(\theta)$.

As in the case without meridional circulation, when β increases at fixed $V(\theta)$ and $v(\theta)$, the cycle duration decreases. The magnetic field amplitude then decays. With increasing β, the amplitude decays more slowly than the slowing down of the dynamo wave propagation.

2.5 Other dynamo models

We note that in addition to the generation of axially symmetric modes of magnetic fields in the $\alpha\Omega$-dynamo model, the possibility of generating nonaxially symmetric modes can be considered. Besides the main $\alpha\Omega$-dynamo approximation, there are α^2- and $\alpha^2\Omega$-dynamo models. In the α^2-model, the effect of differential rotation on magnetic field generation is ignored, and in the $\alpha^2\Omega$-model, the generation of a poloidal field from a toroidal one is due to both differential rotation and the α-effect. However, these models are rather purely academic and are not interesting for the development of asymptotic methods [135–140].

The problem of predominantly nonaxially symmetric magnetic field generation in spiral galaxies, the Sun, and planets like Uranus and Neptune was considered in [135] in the $\alpha\Omega$-dynamo approximation using the maximum effective generation approximation. The hydromagnetic dynamo in these celestial bodies was assumed to be possible in relatively thin conducting convective layers. For predominantly nonaxially symmetric modes to be excited, compared to axially symmetric ones in such layers, the angular velocity gradient in a celestial body should be relatively small and have a significant component normal to the layer.

The WKB method has been applied to the asymptotic study of the $\alpha^2\Omega$-dynamo and α^2-dynamo models (see, e.g., [136–140]).

An asymptotic solution of the system of equations describing the process of the one-dimensional $\alpha^2\Omega$ dynamo in a thin turbulent differentially rotating convective stellar shell was constructed in [136]. Modulation of the dynamo waves related to the local α-effect depending on the latitude and to the radial gradient of the zonal differential matter flow was considered in [137].

3. Low-mode approach in the stellar dynamo. Nonlinear dynamo with dipole and quadrupole magnetic field symmetries for one- and two-layer media

We consider another possible method for obtaining simplified models aimed at clarifying the physics of stellar magnetic field generation. It is assumed that an exited magnetic field can be described by a relatively small number of parameters, which enables substituting dynamo equations with a specially chosen dynamical system of a not very high order. Such a method is referred to as the low-mode approach and was first suggested in [141].

A method for constructing the low-mode description of dynamo equations was developed in [142–146]. In [145], a regular method for constructing a low-mode approximation of dynamo equations is proposed. The low-mode model equations are obtained in the simplest approximation of the algebraic suppression of helicity. As shown in [145], a nonlinear dynamo model obtained in such a way is rich enough and can hopefully describe various aspects of magnetic field generation in spherical shells of celestial bodies (stars and planets).

The simplest system of equations of Parker's dynamo model in the one-dimensional case has the form

$$\frac{\partial A}{\partial t} = R_\alpha \alpha B + \frac{\partial^2 A}{\partial \theta^2}\,, \tag{38}$$

$$\frac{\partial B}{\partial t} = R_\omega \sin\theta\,\frac{\partial A}{\partial \theta} + \frac{\partial^2 B}{\partial \theta^2}\,, \tag{39}$$

where A and B are functions of the latitude θ measured from the pole and time t.

According to [144], the low-mode approximation can be formulated as follows. It is assumed that after the initial growth, the magnetic field in a star is stabilized, its growth stops, and a regime similar to auto oscillations arises. The system here is thought to be rearranged such that the dynamo becomes marginally stable. In this case, it is possible to assume that the solution can be represented as a superposition of a small number of appropriately chosen freely decaying modes. We note that the classic Parker explanation given above represents the dynamo operation in terms of the evolution of two freely decaying modes due to two generation sources, differential rotation and helicity.

It is first necessary to consider the free decay case, where the intensity of generation sources is $R_\alpha, R_\omega = 0$. Here, the eigenfunctions have the form $\{\sin(k\theta), 0\}$, $k = 1, 3, \ldots$ (the dipole symmetry for vector potential A is taken into account) or $\{0, \sin(k\theta)\}$, $k = 2, 4, \ldots$ (the dipole symmetry for the vector potential B is taken into account). The idea of the method is to seek a solution of main equations (38), (39) in the form of a series in the eigenfunctions of the free decay problem; a finite number of terms should be taken. The scalar product of elements x and y is defined as $(x, y) = \int xy\,\mathrm{d}\theta$. Multiplying the first equation by A and the second by B and taking the orthogonality of A and B into account, it is possible to pass to the eigenvalue problem for the matrix W:

$$WC = \lambda C\,. \tag{40}$$

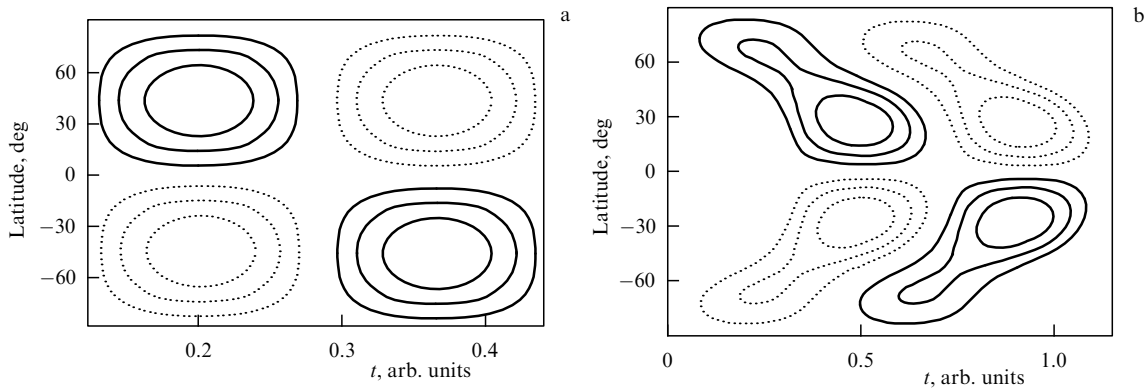

Figure 6. Theoretical butterfly diagrams of the toroidal magnetic field for (a) a fully convective zone and (b) a star with a thin convective shell [146]. The fields with a positive (negative) sign are shown by the solid (dotted) lines. The time is in arbitrary units.

The elements of W are $W_{ij} = \lambda_i^0$ at $i = j$ and

$$W_{ij} = \int \begin{pmatrix} A \\ B \end{pmatrix}_i^* \hat{L} \begin{pmatrix} A \\ B \end{pmatrix}_j ,$$

where λ_i^0 are the eigenvalues of the decay problem, and the operator $\hat{L}$ has the form

$$\hat{L} = \begin{Bmatrix} R_\alpha \cos\theta\,(\cdot) & \dfrac{\partial^2(\cdot)}{\partial\theta^2} \\ \dfrac{\partial^2(\cdot)}{\partial\theta^2} & R_\omega \sin\theta\,\dfrac{\partial(\cdot)}{\partial\theta} \end{Bmatrix}$$

(the dot shows the place where the mode on which the operator acts should be placed). The solution of problem (40) gives eigenfunctions and eigenvalues (growth rates) λ_i. Based on the criterion that the oscillating mode be excited first, it was shown in [144, 145] that four modes (two poloidal and two toroidal) play key roles in the magnetic field generation. By changing the numbers R_α and R_ω, it was found that the leading model generation (with $\operatorname{Re}\lambda \approx 0$) occurs for $R_\alpha = 0.5$ and $R_\omega = 575$ and has $\operatorname{Im}\lambda \approx 7.6\mathrm{i}$, and the expansion coefficients for the toroidal and poloidal field are $C_1^{\mathrm{T}} = 0.72$, $C_2^{\mathrm{T}} = 0.38 + 0.58\mathrm{i}$ and $C_1^{\mathrm{P}} = 0.05 + 0.34\mathrm{i}$, $C_2^{\mathrm{P}} = 0.1 + 0.56\mathrm{i}$.

The critical dynamo number at which the field generation occurs in a fully convective star ($|D| \approx 4500$) is much higher than for Parker's classic dynamo ($|D| \approx 290$). We note that the actual dynamo numbers obtained from numerical simulations of fully convective stars are 3000–5000. It was shown in [144] that properties of solutions of the dynamical system in stars with thin convective shells and in fully convective stars are significantly different. This is due to different decay spectra in different cases. It was shown that unlike the decay spectrum for Parker's classic dynamo, which includes singlets only, the decay spectrum in a fully convective star includes alternate singlets and doublets. It was argued in [144] that the reason standing waves are excited by a dynamo in a fully convective star is that the longitudinal dependence of both modes participating in the generation is proportional to $\sin(2\theta)$, i.e., both modes are fixed at the same latitudes. For Parker's classic dynamo, two modes participate in the field generation with different latitudinal dependences $\sin(2\theta)$ and $\sin(4\theta)$; therefore, the wave can propagate from a maximum of one wave to a maximum of another wave. Figure 6 shows theoretical butterfly diagrams of the toroidal magnetic field for a fully convective star (Fig. 6a) and a star with a thin convective shell (Fig. 6b) [146]. The fields with positive and negative signs are shown by the respective solid and dashed lines. Figure 6 suggests that the wave in the fully convective star is standing, while the one in the star with a thin convective shell is running.

In [144, 146], it was shown that during one activity cycle, spots in stars with thin convective shells and in fully convective stars are distributed differently in latitudes. In addition, for fully convective stars, the model predicts a significant weakening of the spot formation rate at certain phases of the cycle.

The dynamical system studied in [145] was obtained after the substitution in the dynamo equations of the fields with the following latitudinal dependence:

$$A(\theta, t) = a_1(t)\sin\theta + a_2(t)\sin 3\theta ,$$

$$B(\theta, t) = b_1(t)\sin(2\theta) + b_2(t)\sin(4\theta) .$$

The dynamical system has the form

$$\frac{\partial a_1}{\partial t} = \frac{R_\alpha b_1}{2} - a_1 - \xi^2\,\frac{3R_\alpha b_1}{8}(b_1^2 + 2b_2^2) , \tag{41}$$

$$\frac{\partial a_2}{\partial t} = \frac{R_\alpha}{2}(b_1 + b_2) - 9a_2 - \xi^2\,\frac{3R_\alpha(b_1 + b_2)}{8}(b_1^2 + b_1 b_2 + b_2^2) , \tag{42}$$

$$\frac{\partial b_1}{\partial t} = \frac{R_\omega}{2}(a_1 - 3a_2) - 4b_1 , \tag{43}$$

$$\frac{\partial b_2}{\partial t} = \frac{3R_\omega a_2}{2} - 16b_2 . \tag{44}$$

The boundary conditions are used in the form $A(0) = B(0) = A(\pi) = B(\pi) = 0$, which corresponds to the dipole symmetry. In this system, self-excitation is described by linear terms, and stabilization due to the nonlinear suppression of helicity is described by nonlinear terms. The governing parameters are the values R_α and R_ω reduced to the dimensionless form using the turbulent diffusion coefficient and geometrical parameters of the problem that characterize the amplitude of the α-effect and differential rotation.

It is taken into account in Eqns (41)–(44) that the poloidal field is generated by differential rotation and the α-effect is negligible.

In this model, the simplest scheme for the magnetic field growth stabilization is used, the so-called helicity suppression. In this scheme, it is assumed that $\alpha = \alpha_0(\theta)/(1+\xi^2 B^2) \approx \alpha_0(\theta)(1-\xi^2 B^2)$, where $\alpha_0(\theta)$ is the helicity in a nonmagnetized medium and $B_0 = \xi^{-1}$ is the magnetic field at which the α-effect is significantly suppressed. To be specific, we assume that $\alpha_0(\theta) = \cos\theta$.

In [145], solving system of equations (41)–(44) numerically for different R_α and R_ω showed that different generation regimes can be reproduced that resemble the magnetic field behavior in some celestial bodies, including stationary oscillations similar to the solar cycle, dynamo outbursts of the magnetic field observed in laboratory experiments, chaotic perturbations similar to activity in some stars, and vascillations (oscillations around a nonzero value) that are observed in some celestial bodies. The vascillations and chaotic oscillation regime disappear if the variable a_1 is eliminated from the dynamical system.

Analysis of system of equations (41)–(44) showed that the waves describing the toroidal magnetic field propagation are running waves. This is due to the toroidal modes b_1 and b_2 being phase shifted relative to each other, such that the toroidal field propagates along the latitude as a whole. At the same time, the wave characterizing propagation of the poloidal field is virtually standing and barely propagates along the latitude. This is because one of the modes in the poloidal spectrum dominates ($a_2 \gg a_1$).

Observations suggest that the magnetic field of the Sun in most cycles has a prominently dipole symmetry. However, the toroidal field of the Sun in cycles 0 and 1 most likely had the quadrupole and not the dipole symmetry. Butterfly diagrams of the spots for cycles 0 and 1 are presented in [147]. The possibility of a quadrupole structure in cycle 1 is discussed in [148]. Figure 7 shows the butterfly diagram for solar spots for cycles 0–4 [147]. Although the solar magnetic field symmetry is mainly dipole, it is quite possible that the magnetic field of other stars can have not only dipole but also quadrupole symmetry. It is argued in [149] that neither the dynamo theory nor observations support the hypothesis that stellar magnetic fields should have only the dipole symmetry with respect to the stellar equator. In addition, in [149], the simplest migration dynamo models were studied numerically, and magnetic field generation regimes with nondipole symmetry and transitions from one symmetry to another were found.

A dynamical model based on the $\alpha\Omega$ dynamo for the quadrupole symmetry of the magnetic field was constructed in [150].

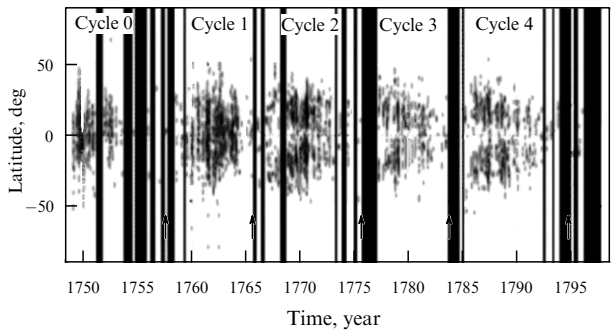

Figure 7. Butterfly diagram of solar spots for cycles 0–4 [147].

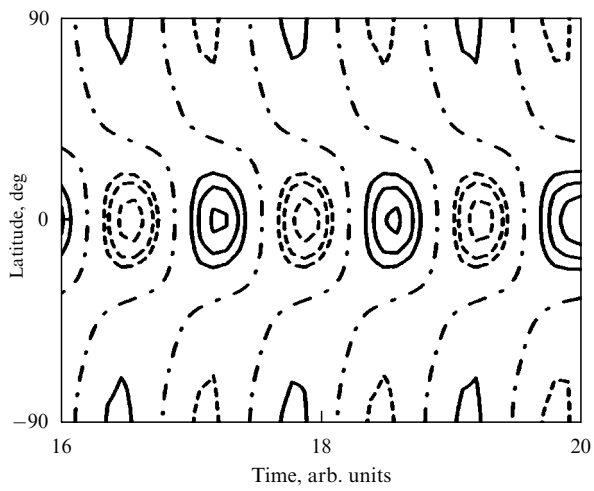

Figure 8. Latitude–time distribution of the toroidal field for $D = -120$. The solid and dashed lines show the respective positive and negative magnetic fields. Time is in arbitrary dimensionless units. The dashed-dotted lines mark zero-level lines [150].

In the case of the quadrupole symmetry of the magnetic field, the oscillation regime arises not only when one poloidal and two toroidal modes are taken into account, as in the case of dipole symmetry, but also when two poloidal and one toroidal modes are taken into account.

According to [150], in the oscillation regime, an increase in the dynamo number leads to magnetic field growth near the equator and near the poles. In the theoretical butterfly diagrams for the toroidal field, the near-equatorial region appears in the form of spot clusters at the equator for solar activity cycles 0 and 1 (see [147]). Figure 8 shows the time–latitude distribution of the toroidal field in the oscillation regime. The isocurves of the positive and negative field are respectively shown by solid and dashed lines. The time is measured in arbitrary dimensionless units. The dashed–dotted lines indicate the zero field lines. We note that the range of dynamo numbers in which the magnetic field oscillation with dipole symmetry is possible lies inside the range for the oscillation regime with the quadrupole symmetry of the field.

Using the dynamical system obtained in the low-mode approximation, a quasi-two-year solar activity cycle was modeled [151–154]. Based on the analysis of observations, it was shown in [155–164] that quasi-cyclic bursts of magnetic activity occur every 0.5–2.0 years on top of the 22-year solar cycle. Using a wavelet analysis of large-scale magnetic field data in 1960–2000, the two-year oscillations were shown to be quite chaotic; however, waves propagating toward the poles can also be distinguished in this cycle. To explain the double cycle of solar activity, the authors of [165] proposed using Parker's model for a two-layer medium [32]. The formation of low-frequency oscillations in the convective zone is due to the large-scale radial shear $\partial\Omega/\partial r$ of the angular velocity Ω, and the high-frequency component of the cycle can appear due to the latitudinal shear $\partial\Omega/\partial\theta$ or radial shear of the angular velocity ω in the near-surface region of the convective zone. However, the mixed cycle can also appear for other reasons. Within the low-mode approximation, it was demonstrated in [151, 152] that if three or more modes of toroidal and poloidal fields are taken into account in the latitudinal distribution, a regime similar to the

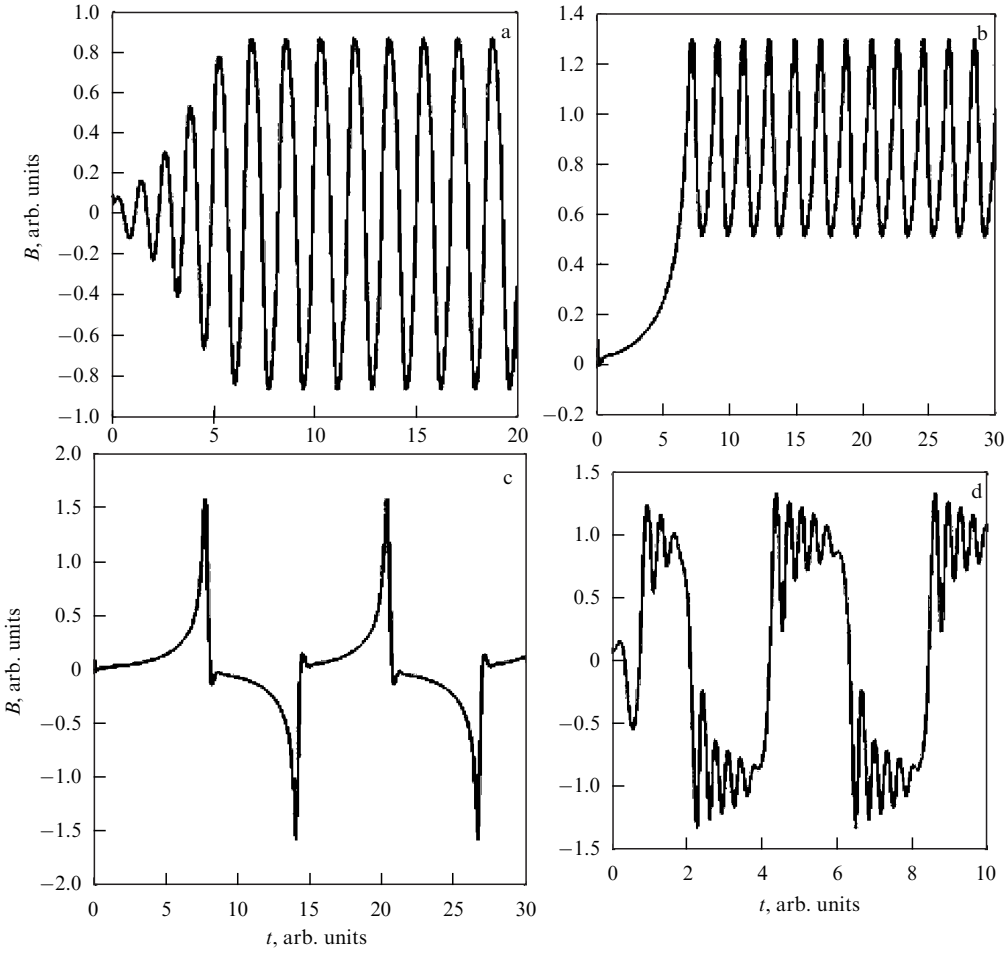

Figure 9. Regimes for generating the leading mode of the toroidal field that appeared in the models described: (a) oscillation regime, (b) vascillation regime, (c) dynamo bursts, (d) simultaneous presence of the 22-year and quasi-two-year cycles. The field amplitude is plotted as a function of time (both in arbitrary units).

coexistence of the 22-year and quasi-two-year cycles appears. Such a regime can be reproduced for realistic solar parameters (dynamo numbers, thickness of the solar convective zone, meridional flows).

To model the double cycle of solar activity using the low-mode approximation, a two-layer dynamo model was constructed in [153, 154] under the assumption that the motion of a dynamo wave in the upper layer of the convective zone breaks down due to meridional flows directed opposite to the toroidal magnetic field propagation, and dynamo wave propagation in deeper layers coincides with the meridional flow direction, and the period of the wave is shorter than in the upper layer. Parameter ranges (dynamo numbers and meridional circulation) were found in the cases where the double cycle (simultaneous presence of the 22-year and quasi-two-year cycles) and the triple cycles (simultaneous presence of the secular, 22-year, and quasi-two-year cycles) appear. In [153], the triple cycle was shown to be possibly due to the appearance of a regime with two harmonics in each layer and beats.

Figure 9 shows different regimes for generating the leading mode of the toroidal field that appeared in the described models. Figure 9a presents the oscillation regime, Fig. 9b shows the vascillation regime, Fig. 9c shows dynamo bursts, and Fig. 9d shows a cycle with the simultaneous presence of the secular, 22-year, and quasi-two-year cycles. The field amplitude is along the ordinate and the time is along the abscissa, both in arbitrary dimensionless units.

4. Asymptotic methods to study the galactic dynamo model

4.1 Semiclassical approximation for the dynamo in a thin disk (axially symmetric solutions)

Some galaxies (for example, the Andromeda galaxy M31) have a ring-like magnetic field distribution at about 10 kpc from the galactic center. Other galaxies, for example M33 and M51, show a distinctly bisymmetric spiral-like field structure (Fig. 10). The field configuration in some galaxies is more complicated; for example, it can be close to an axially symmetric form in the central parts and bisymmetric in the outer parts of the galaxy.

Figure 11 shows magnetic fields in the galaxy M51. The magnetic field was inferred from measurements at 6 cm by the 100 m Effelsberg telescope and by the VLA (USA). The contour lines show the observed radio emission, to which the magnetic field strength is proportional; the dashes indicate the magnetic field direction. The optical image was obtained by the Hubble Space Telescope.

Dynamo models for the mean field of spiral galaxies were first suggested in [166–168]. These models are local and the

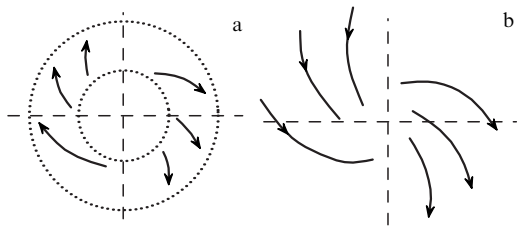

Figure 10. (a) Axially symmetric and (b) bisymmetric structures of galactic magnetic fields.

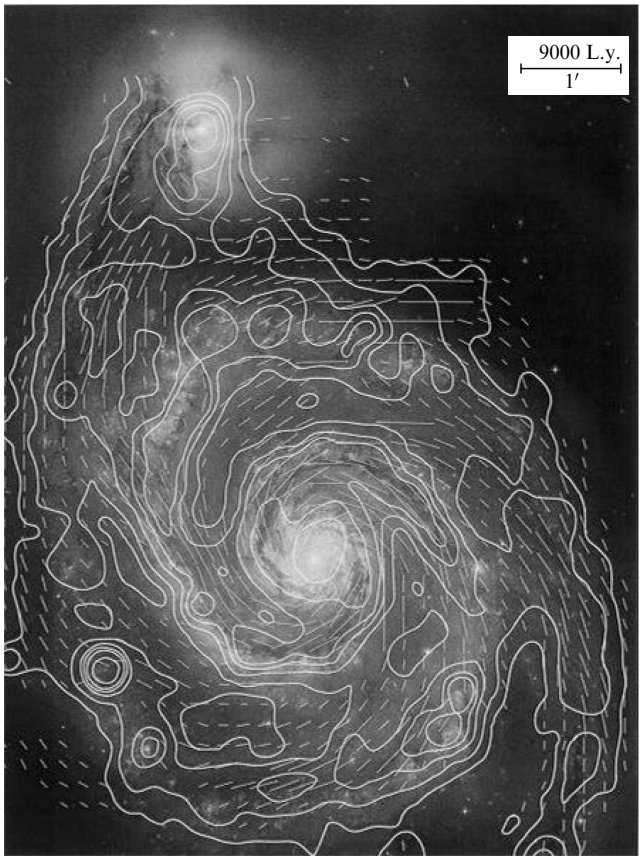

Figure 11. Magnetic fields in the spiral galaxy M51. The contour lines show the total radio emission, to which the magnetic field strength is proportional. The optical image is obtained by the Hubble Space Telescope.

derivatives are constant across the disk. Later, the galactic dynamo theory was extended to the two- and three-dimensional cases and applied to different types of galaxies [19, 20, 169]. Such models allow an asymptotic analysis. In [61, 62, 170, 171], exact asymptotic solutions of the $\alpha\Omega$-dynamo models in thin disks were found.

Usually, galactic dynamo models are formulated in a thin differentially rotating turbulent disk surrounded by a vacuum. The dynamo equations are written in cylindrical coordinates (r, φ, z) centered at the disk center, with the z axis parallel to the galactic angular velocity. The models are formulated in dimensionless units: r and z are measured in units of the disk radius r_0 and disk half-thickness h_0. A typical r_0 is 8.5 kpc, and h_0 is about 0.5 kpc. The time is measured in units of the turbulent magnetic diffusion time across the disk, h_0^2/β. The typical diffusion time is about 7.5×10^8 years.

The axially symmetric magnetic field has three components, which are expressed in terms of the azimuthal component of the large-scale magnetic field B_φ and the vector potential A_φ:

$$B = \left(-\frac{\partial A_\varphi}{\partial z},\, B_\varphi,\, \frac{1}{r}\frac{\partial}{\partial r}(rA_\varphi)\right). \tag{45}$$

Magnetic field generation equations in the dimensionless units are

$$\frac{\partial B_\varphi}{\partial t} = -R_\omega g\,\frac{\partial A_\varphi}{\partial z} + \frac{\partial^2 B_\varphi}{\partial z^2} + \varepsilon^2\,\frac{\partial}{\partial r}\left(\frac{1}{r}\frac{\partial}{\partial r}(rB_\varphi)\right), \tag{46}$$

$$\frac{\partial A_\varphi}{\partial t} = R_\alpha \alpha B_\varphi + \frac{\partial^2 A_\varphi}{\partial z^2} + \varepsilon^2\,\frac{\partial}{\partial r}\left(\frac{1}{r}\frac{\partial}{\partial r}(rA_\varphi)\right), \tag{47}$$

where R_α and R_ω are turbulent magnetic Reynolds numbers characterizing amplitudes of the mean helicity and differential rotation. It is assumed in Eqns (46) and (47) that the differential rotation does not depend on z; in addition, the contribution of the mean helicity α to the magnetic field generation is ignored in (46). There, $g = r\,\mathrm{d}\Omega/\mathrm{d}r$ is the measure of the differential rotation. In the solar vicinity of the Galaxy, the mean helicity, differential rotation, and turbulent diffusion coefficient are $\alpha_0 \approx 10^5$ cm s^{-1}, $g_0 \approx 10^{-15}$ s^{-1}, and $\beta \approx 10^{26}$ cm^2 s^{-1}. In Eqns (46) and (47), $D = R_\alpha R_\omega$ is the dimensionless dynamo number and $\varepsilon^2 = h_0^2/r_0^2 \approx 10^{-3}$ is a small parameter due to the large difference between the vertical and horizontal sizes of the disk. Due to this difference, the magnetic field relatively rapidly diffuses in the z-direction normal to the disk plane in $h_0^2/\beta \approx 5 \times 10^8$ years and slowly diffuses along the radius in $r_0^2/\beta \approx 5 \times 10^{11}$ years. We note that the age of galaxies does not exceed 10^{10} years.

The kinematic axially symmetric asymptotic solution in this case has the form

$$\begin{pmatrix} B_\varphi \\ A_\varphi \end{pmatrix} = \exp(\Gamma t)\left[Q(\varepsilon^{-1/3}r)\begin{pmatrix} \tilde{B}(r,z) \\ \tilde{A}(r,z) \end{pmatrix} + \ldots\right], \tag{48}$$

where $\Gamma = \mathrm{d}\ln B/\mathrm{d}t$ is the growth rate of different modes of the field, $(\tilde{B}, \tilde{A})$ are normalized functions, and Q is the amplitude of the solution, which can be found for a given radius.

The local solution (for a fixed point r) occurs in the lowest order of the expansion in ε. This solution corresponds to a system of equations that can be derived from (46), (47) by setting $\varepsilon = 0$. Such a system contains only derivatives with respect to z with coefficients parametrically dependent on r:

$$\gamma(r)\tilde{B} = -R_\omega g(r)\,\frac{\partial \tilde{A}}{\partial z} + \frac{\partial^2 \tilde{B}}{\partial z^2}, \tag{49}$$

$$\gamma(r)\tilde{A} = R_\alpha \alpha(r,z)\tilde{B} + \frac{\partial^2 \tilde{A}}{\partial z^2}. \tag{50}$$

Here, $\gamma(r)$ is the local growth rate.

Boundary conditions frequently used on the disk surface $z = \pm h(r)$ correspond to the vacuum outside the circle. For axially symmetric fields in the lowest order in ε, we have

$$\tilde{B} = 0, \qquad \frac{\partial \tilde{A}}{\partial z} = 0 \tag{51}$$

at $z = \pm h(r)$. Because α is an odd function of z, the generated waves have either quadrupole or dipole symmetry. The

symmetry character is determined by the conditions [19]

$$\tilde{A} = 0\,, \qquad \frac{\partial \tilde{B}}{\partial z} = 0 \tag{52}$$

at $z = 0$ (the quadrupole symmetry) and

$$\tilde{B} = 0\,, \qquad \frac{\partial \tilde{A}}{\partial z} = 0 \tag{53}$$

at $z = 0$ (the dipole symmetry).

To explore the behavior of modes of the magnetic field waves in a thin disk, we consider Eqns (49) and (50) in the form of an expansion in freely decaying modes, i.e., without field generation sources at R_α and $R_\omega = 0$:

$$\gamma_n \tilde{B}_n = \frac{\partial^2 \tilde{B}_n}{\partial z^2}\,, \tag{54}$$

$$\gamma_n \tilde{A}_n = \frac{\partial^2 \tilde{A}_n}{\partial z^2}\,. \tag{55}$$

Here, γ_n is the decay rate of the nth mode; we note that $\gamma_n < 0$. We consider the quadrupole boundary conditions; then an orthonormal basis of functions is given by

$$\begin{pmatrix} \tilde{B}_{2n} \\ \tilde{A}_{2n} \end{pmatrix} = \begin{pmatrix} \sqrt{2}\cos\left(\pi\left(n+\dfrac{1}{2}\right)\dfrac{z}{h}\right) \\ 0 \end{pmatrix}, \tag{56}$$

$$\begin{pmatrix} \tilde{B}_{2n+1} \\ \tilde{A}_{2n+1} \end{pmatrix} = \begin{pmatrix} 0 \\ \sqrt{2}\sin\left(\pi\left(n+\dfrac{1}{2}\right)\dfrac{z}{h}\right) \end{pmatrix}, \tag{57}$$

$$\gamma_{2n} = \gamma_{2n+1} = -\pi^2\left(n+\frac{1}{2}\right)^2, \qquad n = 0, 1, \ldots\,. \tag{58}$$

The eigenvalues are doubly degenerate. The solution of Eqns (49) and (50) in this case can be represented in the form

$$\begin{pmatrix} \tilde{B} \\ \tilde{A} \end{pmatrix} \approx \exp(\gamma t) \sum_{n=0}^{\infty} c_n \begin{pmatrix} \tilde{B}_n \\ \tilde{A}_n \end{pmatrix}, \tag{59}$$

where c_n are constants. After substituting the obtained series in (49) and (50), multiplying by $(\tilde{B}_k, \tilde{A}_k)$, and integrating over z from 0 to h, we obtain an algebraic system of homogeneous equations for c_n, whose solvability condition gives an algebraic equation for γ. To analyze the behavior of waves, it suffices to consider a minimal set of modes generating the magnetic field. In this problem, the minimal number of modes is two; therefore, we obtain a system of two equations for c_0 and c_1 and a quadratic equation for γ. The positive solution of this equation for γ is

$$\gamma = -\frac{1}{4}\pi^2 + \mathrm{i}\sqrt{R_\alpha R_\omega \int_0^h \alpha b_0 a_1\,\mathrm{d}z \int_0^h b_0 a_1\,\mathrm{d}z}\,. \tag{60}$$

In the case $\alpha = \sin(\pi z/h)$, we have $\gamma = -\pi^2/4 + \mathrm{i}\sqrt{D/\pi}$. To assess the accuracy of Eqn (60), we obtain $\gamma = 0$ for $D = D_{\mathrm{cr}} = -\pi^5/16 \approx -19$. The precise value was obtained in [19] and is $D_{\mathrm{cr}} = -8$. This solution suggests that the dominant mode does not oscillate ($\mathrm{Im}\,\gamma = 0$).

For the dipole symmetry, we similarly find $\gamma = -n^2\pi^2$, $n = 1, 2, \ldots$. Therefore, the lowest dipole mode decays four times as fast as the lowest quadrupole mode. The reason is that the azimuthal field with dipole symmetry vanishes not only at $|z| = h$ but also at $z = 0$ and hence has a smaller scale than the quadrupole solution. This immediately implies that the quadrupole modes should dominate in galactic disks. We note that the dominant symmetry in galaxies differs from the dominant symmetry in stars and planets, in which the field with the dipole symmetry prevails. This result is supported by observations.

In galactic dynamo problems, vacuum boundary conditions are frequently used because of their relative simplicity. In addition, they are local in the lowest order in the expansion in ε. However, this advantage is lost when a higher-order expansion in ε is required to obtain the radial field distribution. In that case, the magnetic field lines can go out of the disk at one radius, pass through the ambient vacuum, and return to the disk at another radius. For radius-dependent dynamo equations, the vacuum conditions should be formulated for the first-order expansion in ε.

If a galactic disk is immersed in the vacuum, electric fields outside the disk are absent and hence the magnetic field potential is $\mathbf{B} = -\nabla\Phi$. By virtue of the axial symmetry, the axial field outside the disk vanishes. Because the magnetic field must be continuous at the disk boundary, the boundary condition on the disk surface $z = \pm h(r)$ is

$$B_\varphi\Big|_{z=\pm h} = 0\,. \tag{61}$$

Vacuum boundary conditions for the poloidal field in local Cartesian coordinates were obtained in [60]. In cylindrical coordinates, they take the form [170]

$$\frac{\partial A_\varphi}{\partial z} - \frac{\varepsilon}{r} L(A_\varphi) = 0 \tag{62}$$

at $z = \pm h(r)$, where

$$L(A_\varphi) = \int_0^\infty W(r, r')\,\frac{\partial}{\partial r'}\left(\frac{1}{r'}\frac{\partial}{\partial r'}\,r' A_\varphi\right)\mathrm{d}r'\,,$$

$$W(r, r') = rr' \int_0^\infty J_1(kr) J_1(kr')\,\mathrm{d}k\,,$$

and $J_1(x)$ are the Bessel functions. In [171], another equivalent form of the integral operator $L(A_\varphi)$ was obtained that included the Green's function for the Neumann problem for the Laplace equation.

The integral part of the boundary condition can be rearranged to a nonlocal term in the equation for Q. This equation becomes an integro-differential equation of the form [170]

$$\big[\Gamma - \gamma(r)\big]\,q(r) = \varepsilon p(r) L\big(q(r)\big)\,, \tag{63}$$

where

$$q(r) = Q(r)\tilde{A}(h, r)\,,$$

$$p(r) = \frac{\tilde{A}(h, r)\tilde{A}_*(h, r)}{\langle Y, Y_*\rangle}\,, \qquad Y = \begin{pmatrix} \tilde{B}(r, z) \\ \tilde{A}(r, z) \end{pmatrix}.$$

Here, the asterisk denotes an eigenvector for the adjoint problem and $\langle Y, Y_*\rangle = \int_0^h Y\,Y_*\,\mathrm{d}z$.

The solution of Eqn (63) with boundary conditions $q(0) = 0$ and $q \to 0$ as $r \to 0$ is another boundary value problem for which the growth rate Γ is an eigenvalue and the eigenfunction $q(r)$ determines the radial profile of the eigenfunction Q. In [171], the contribution of the integral term to Eqn (63) was described as an extension of radial diffusion.

4.2 Adiabatic approximation for the galactic dynamo model

Equation (63) was simplified in [172] and [19] by neglecting the term with ε in boundary condition (62). This makes the boundary condition local and results in an equation for $Q(r)$,

$$\left[\Gamma - \gamma(r)\right] Q = \varepsilon^2 \frac{\partial}{\partial r}\left(\frac{1}{r}\frac{\partial}{\partial r} rQ\right), \tag{64}$$

which is similar to (63), but has the integral term replaced with the diffusion operator. Here, $\gamma(r)$ is an analog of the potential in quantum mechanics. This approach is similar to the adiabatic approximation in quantum theory, which is valid for $\Delta\Gamma \ll \Delta\gamma(r)$, where $\Delta\Gamma$ is the spacing between the corresponding eigenvalues. For the galactic disk, this condition is satisfied: $\Delta\Gamma \leqslant 0.4$, $\Delta\gamma \approx 1$.

The adiabatic approximation ignores any local coupling between different parts of the disk through the halo, but includes the local diffusion coupling inside the disk. This simplification significantly facilitates the asymptotic analysis of dynamo problem solutions in the thin disk approximation for galaxies and accretion disks, with nonlocal effects neglected. Equation (63) can be solved analytically or numerically [19], but some features of the solution are lost when neglecting nonlocal effects. The most serious inaccuracy is that the asymptotic scaling of the solution depends on ε, and here the radial scale becomes $\varepsilon^{-1/2}h_0$ instead of the true value $\varepsilon^{-1/3}h_0$. However, this difference is hardly essential for the actual values $\varepsilon \sim 10^{-1} - 10^{-2}$. We note that the asymptotic behavior in the thin disk approximation is sufficiently accurate for $\varepsilon < 10^{-1}$ [171, 172].

In [173], the adiabatic approximation is applied to calculate the turbulent MHD dynamo of magnetic fields in thin disks. The adiabatic method is used to study conditions under which magnetic fields generated in the disk penetrate the entire disk or are localized in bounded domains. The problem is considered for two particular cases of Keplerian disks. In the first case, magnetic field diffusion is assumed to dominate because of turbulent mixing, and consequently the dynamo number is assumed to be independent of the distance to the disk center. In the second case, the dynamo number can vary with the distance from the disk center. The magnetic field localization turns out to be a general property of dynamos in disks, except for a special case of a steady-state dynamo with a constant dynamo number. The consequences of this feature for dynamic behavior of a dynamo in magnetized accretion disks are discussed in [173]. Results of these calculations are tested in models of the proto-solar cloud and accretion disks around compact objects.

Nonlocal effects also manifest themselves as the appearance of power-law asymptotic solutions of Eqn (63): far from the active dynamo region, $q \sim r^{-4}$, whereas solutions of Eqn (64) have an exponential asymptotic behavior typical for the diffusion equation. This affects the propagation velocity of magnetic fronts during the kinematic growth of a magnetic field: with nonlocal effects taken into account, the fronts propagate exponentially, while the local radial diffusion leads only to linear propagation.

Ignoring nonlocal effects does not significantly affect the observed quantities. We note that parameters of spiral galaxies and their magnetic fields are known with limited accuracy. In addition, halos of spiral galaxies can be treated as a vacuum only very approximately. The final conductivity of the halo weakens the nonlocal effects.

The theory described above can be extended to the case of nonaxisymmetric solutions. In [19, 174, 175], asymptotic solutions are constructed using the WKB method for a galactic dynamo with $|D| \gg 1$. Such asymptotic solutions of one-dimensional dynamo equations (49) and (50) are discussed in [33].

4.3 Semiclassical approximation for a nonlinear dynamo

Nonlinear asymptotic solutions of Eqns (49) and (50) with $|D| \gg 1$ are constructed in [176] by assuming that the nonlinearity significantly affects the magnetic field distribution across the disk, and that the steady-state dynamo sets in locally in the lowest approximation. The radial coupling is significant already at the kinematic stage, where it gives rise to a global eigenfunction according to (63) or (64). Nonlinear effects most likely affect the global eigenfunciton and therefore should alter the radial equation. In [177], a nonlinear analog of Eqn (64) was derived with algebraic suppression of the helicity α:

$$\tilde{\alpha} = \frac{\alpha}{1 + \bar{B}^2/B_0^2}, \tag{65}$$

where B_0 is the saturation level, most frequently identified with the state in which the magnetic and turbulent kinetic energy densities are of the same order. As a result, the magnetic field can increase when $\bar{B} \ll B_0$. When $\bar{B}$ approaches B_0, the field growth slows down, because the α-effect amplitude decreases. A nonlinear asymptotic model of a thin disk can be constructed by replacing $\gamma(r)$ in (63) and (64) with $\gamma(r)(1 - Q^2/B_0^2)$. In this case, Eqn (64) with nonlinearity (65) takes the form

$$\frac{\partial Q(r)}{\partial t} = \gamma(r)\left(1 - \frac{Q^2(r)}{B_0^2}\right)Q(r) + \varepsilon^2 \frac{\partial}{\partial r}\left(\frac{1}{r}\frac{\partial}{\partial r} rQ(r)\right) \tag{66}$$

if the local solution is normalized such that Q is the field strength averaged across the disk at a given radius. In [177], this equation was derived by averaging dynamo equations in the disk. Equation (66) and its nonaxially symmetric variant are widely used to model the galactic dynamo (see, e.g., [20]).

The precise physical mechanism of dynamo saturation remains unknown. In [178], the saturation mechanism is related to suppression of the Lagrangian chaos in gas flows by a magnetic field. This mechanism seems to be reasonable for convective systems (where flows become random for internal reasons, for example, due to instabilities) and can hardly effectively apply to galaxies, where the flow is random due to the randomness of the external force (supernova explosions).

In [179, 180], numerical solutions of galactic dynamo equations were obtained that extend the thin-disk approximation and are based on the 'embedded disk' approach. Instead of using complicated boundary conditions on the disk surface, the disk is considered to be embedded into a halo large enough to make the boundary conditions at the remote halo boundaries insignificant. Because the turbulent magnetic diffusion in galactic halos is larger than in galactic disks [177, 181], the 'embedded disk' models match the asymptotic solutions in the thin-disk approximation obtained with vacuum boundary conditions and confirm the asymptotic results. The 'embedded disk' approach has also been used to study galactic halos in which the dynamo mechanism operates intensively [182–185]. Later dynamo models in the

disk were constructed that take magnetic buoyancy effects [186], accretion flows [187], and external magnetic fields [188, 189] into account.

In nonlinear dynamo models for thin disks, the local solution does not depend on nonlinear effects, which mainly alter the radial field structure. Consequently, the inclination angle of magnetic field lines ($p = \arctan(B_s/B_\varphi)$) is expected to be only weakly changed by nonlinear effects. This is an important feature of the solution, which can be compared to observations [172]. However, the influence of nonlinear effects on the inclination of magnetic field lines has never been explored in detail.

4.4 No-z approximation to study the galactic dynamo model

The no-z approximation was proposed for thin galactic disks and developed in [190–192]. The main property of this approximation is the change in the magnetic field derivatives along the direction normal to the disk plane by the magnetic field value divided by the disk half-thickness h or h^2. The no-z approximation widely applies to explain galactic magnetic fields. Dynamo equations (46) and (47) in a galactic disk in cylindrical coordinates (r, φ, z) with the origin in the disk center in this approximation have the form

$$\frac{\partial B_\varphi}{\partial t} = R_\omega r \frac{\partial \Omega}{\partial r} B_r - \frac{\pi^2}{4} B_\varphi + \lambda \frac{\partial}{\partial r}\left(\frac{1}{r}\frac{\partial}{\partial r}(rB_\varphi)\right), \quad (67)$$

$$\frac{\partial B_r}{\partial t} = -R_\alpha B_\varphi - \frac{\pi^2}{4} B_r + \lambda \frac{\partial}{\partial r}\left(\frac{1}{r}\frac{\partial}{\partial r}(rB_r)\right). \quad (68)$$

The radial field B_r is obtained from the azimuthal field B_φ by the α-effect, and the azimuthal field is obtained from the radial field by the differential rotation. These fields are subjected to the turbulent diffusion η and general rotation Ω, $\lambda = h/R$. The third magnetic field component is recovered from the solenoidality condition. The time is measured in units of h^2/η and the distance in units of the galactic radius r_0; the angular velocity is normalized to the characteristic value Ω_0, and the characteristic numbers $R_\alpha = \alpha_0 h/\eta$, $R_\omega = \Omega_0 h^2/\eta$ are introduced such that $D = R_\alpha R_\omega$.

Equations (67) and (68) are usually solved by the WKB method or numerically. Such an approach, at first glance, seems to be rather crude; however, it is quite effective, because the magnetic field structure across a thin disk is sufficiently simple, at least for the lowest mode. Increasing the accuracy of the approximation is discussed in [192]. In [190], this model was applied to the effect of spiral arms of galactic magnetic fields.

As shown in [192], the asymptotic study of linear dynamo equations (67), (68) and (46), (47) for the Brandt differential rotation for the M31 galaxy (in the region where the thin disk approximation is applicable) gives close results. The eigenfunctions in the linear approximation for these cases are the same. The magnetic field growth rates for the two approximations are different, but the correction coefficient remains the same (within a 1% accuracy) unless the dynamo number is too large. The introduction of the factor $\pi^2/4$ and change in α_0 in the no-z approximation from 1 to $2/\pi$ improve the results. In addition, the discrepancy can be compensated by changing R_α, because this value has not been precisely determined yet.

Nonlinear equations of the galactic dynamo with the algebraic suppression of helicity are more realistic. The deviation between the solutions of Eqns (67), (68) and (46), (47) in the nonlinear case is larger than in the linear case for not large dynamo numbers and is rather significant for high dynamo numbers.

In [193], it was assumed that the dynamo mechanism works more effectively in the material arms of galaxies, and a retardation mechanism acts on the generated magnetic field. It was found that this results in magnetic field generation between the arms. To obtain asymptotically correct solutions, the WKB method was used with the retardation effect taken into account. Using local equations of the no-z approximation, explicit expressions for the magnetic field growth rate and its radial and azimuthal distributions were obtained.

Local and global asymptotic nonaxially symmetric solutions of Eqns (67) and (68) were constructed in [193], which we do not present here due to their complexity. In [193], the mean-field dynamo theory was extended in two directions. First, semi-analytic solutions for axially symmetric and dominating nonaxially symmetric components ($m = 0$ and $m = \pm 2$ for a two-arm α-spiral) were obtained. Second, effects of the final relaxation time τ of the mean electromotive force related to the final correlation time of a random flow were investigated.

The asymptotic results obtained in [193] were confirmed numerically in [194].

5. Conclusion

The papers reviewed here show that the use of asymptotic expansions yields realistic results consistent with observations. The use of asymptotic methods allows obtaining the analytic dependences of different characteristics of magnetic field waves as functions of different control parameters of the models. This clarifies to which extent one physical factor or another is able to affect the magnetic activity of a celestial body. Such estimates can be used to test complex numerical modeling.

Thus, asymptotic methods are an effective tool to study the problems of generation and evolution of magnetic fields. In addition, the results of asymptotic studies are useful in testing numerical algorithms.

The author thanks D D Sokoloff for the useful discussions. The work was supported by the Russian Science Foundation grant 16-17-10097.

References

1. Gilberti W *De Magnete, Magneticisque Corporibus, et de Magno Magnete Tellure. Physiologia Nova, Plurimis & Experimentis Demonstrata* (Londoni: Petrus Short, 1600); Translated into English: *De Magnete* (New York: Dover Publ., 1958); Translated into Russian: *O Magnite, Magnitnykh Telakh i o Bol'shom Magnite — Zemle. Novaya Fiziologiya, Dokazannaya Mnozhestvom Argumentov i Opytov* (Moscow: Izd. AN SSSR, 1956)
2. Hale G E *Astrophys. J.* **28** 315 (1908)
3. Babcock H W *Astrophys. J.* **105** 105 (1947)
4. Alfvén H *On the Origin of the Solar System* (Oxford: Clarendon Press, 1954)
5. Alfvén H *Rev. Geophys. Space Phys.* **15** 271 (1977)
6. Alfvén H *Ark. Mat. Astron. Fys.* **27A** 1 (1937)
7. Chandrasekhar S, Fermi E *Astrophys. J.* **118** 113 (1953)
8. Ginzburg V L *Usp. Fiz. Nauk* **51** 343 (1953)
9. Ginzburg V L *Sov. Phys. Dokl.* **9** 329 (1964); *Dokl. Akad. Nauk SSSR* **156** 43 (1964)
10. Ginzburg V L *The Propagation of Electromagnetic Waves in Plasmas* (Oxford: Pergamon Press, 1970); Translated from Russian: *Rasprostranenie Elektromagnitnykh Voln v Plazme* (Moscow: Nauka, 1967)

11. Ginzburg V L, Ozernoi L M *Sov. Phys. JETP* **20** 689 (1965); *Zh. Eksp. Teor. Fiz.* **47** 1030 (1964)
12. Ginzburg V L, Syrovatskii S I *The Origin of Cosmic Rays* (Oxford: Pergamon Press, 1964); Translated from Russian: *Proiskhozhdenie Kosmicheskikh Luchei* (Moscow: Izd. AN SSSR, 1963)
13. Ginzburg V L, Usov V V *JETP Lett.* **15** 196 (1972); *Pis'ma Zh. Eksp. Teor. Fiz.* **15** 280 (1972)
14. Ginzburg V L, Zheleznyakov V V *Annu. Rev. Astron. Astrophys.* **13** 511 (1975)
15. Hiltner W A *Astrophys. J.* **128** 9 (1958)
16. Schmidt Th *Astron. Astrophys.* **6** 294 (1970)
17. Mathewson D S, Ford V L *Astron. J.* **75** 778 (1970)
18. Beck R *Astron. Astrophys.* **106** 121 (1982)
19. Ruzmaikin A A, Shukurov A M, Sokoloff D D *Magnetic Fields of Galaxies* (Astrophysics and Space Science Library, Vol. 133) (Dordrecht: Kluwer Acad. Publ., 1988)
20. Beck R et al. *Annu. Rev. Astron. Astrophys.* **34** 155 (1996)
21. Beck R, Wielebinski R "Magnetic fields in galaxies", in *Planets, Stars and Stellar System* Vol. 5 *Galactic Structure and Stellar Populations* (Dordrecht: Springer, 2013) p. 641
22. Schubert G, Soderlund K M *Phys. Earth Planet. Interiors* **187** 92 (2011)
23. Larmor J *Rep. Brit. Assoc. Adv. Sci.* 159 (1919)
24. Cowling T G *Mon. Not. R. Astron. Soc.* **94** 39 (1934)
25. Herzenberg A *Philos. Trans. R. Soc. Lond.* **250** 543 (1958)
26. Backus G *Ann. Physics* **4** 372 (1958)
27. Parker E N *Astrophys. J.* **122** 293 (1955)
28. Vitinskii Yu I *Solnechnaya Aktivnost'* (Solar Activity) (Moscow: Nauka, 1983)
29. Babcock H W *Astrophys. J.* **133** 572 (1961)
30. Leighton R B *Astrophys. J.* **156** 1 (1969)
31. Krause F, Rädler K-H *Mean-Field Magnetohydrodynamics and Dynamo Theory* (New York: Pergamon Press, 1980); Translated into Russian: *Magnitnaya Gidrodinamika Srednikh Polei i Teoriya Dinamo* (Moscow: Mir, 1984)
32. Parker E N *Astrophys. J.* **408** 707 (1993)
33. Zel'dovich Ya B, Ruzmaikin A A, Sokoloff D D *Magnetic Fields in Astrophysics* (New York: Gordon and Breach, 1983); Translated into Russian: *Magnitnye Polya v Astrofizike* (Moscow – Izhevsk: Inst. Komp'yut. Issled., RKhD, 2006)
34. Dormy E, Soward A M (Eds) *Mathematical Aspects of Natural Dynamos* (New York: CRC Press/Taylor and Francis, 2007)
35. Roberts P H, Soward A M *Annu. Rev. Fluid Mech.* **24** 459 (1992)
36. Soward A M *Adv. Space Res.* **12** 257 (1992)
37. Braginsky S I *Geomagn. Aeron.* **7** 851 (1967); *Geomagn. Aeronomiya* **7** 1050 (1967)
38. Cowling T G *Magnetohydrodynamics* (New York: Interscience Publ., 1957)
39. Braginskii S I *Sov. Phys. JETP* **20** 726 (1965); *Zh. Eksp. Teor. Fiz.* **47** 1084 (1964)
40. Braginskii S I *Sov. Phys. JETP* **20** 1462 (1965); *Zh. Eksp. Teor. Fiz.* **47** 2178 (1964)
41. Seehafer N, Pipin V *Astron. Astrophys.* **508** 9 (2009)
42. Elsasser W M *Phys. Rev.* **69** 106 (1946)
43. Roberts P H, in *Mathematical Problems in the Geophysical Sciences* Vol. 2 (Lectures in Applied Mathematics, Vol. 14, Ed. W H Reid) (Providence, RI: American Mathematical Society, 1971) p. 129
44. Roberts P H, Soward A M *Astron. Nachr.* **296** 49 (1975)
45. Yoshimura H *Astrophys. J. Suppl.* **29** 467 (1975)
46. Yoshimura H *Astrophys. J.* **201** 740 (1975)
47. Yoshimura H *Astrophys J.* **226** 706 (1978)
48. Yoshimura H *Astrophys J.* **227** 1047 (1979)
49. Zel'dovich Ya B *Zh. Eksp. Teor. Fiz.* **7** 1466 (1937)
50. Zel'dovich Ya B *Sov. Phys. JETP* **4** 460 (1957); *Zh. Eksp. Teor. Fiz.* **31** 154 (1956)
51. Zel'dovich Ya B *Sov. Phys. JETP* **21** 656 (1965); *Zh. Eksp. Teor. Fiz.* **48** 986 (1965)
52. Zel'dovich Ya B *Astrophysics* **6** 164 (1970); *Astrofiz.* **6** 319 (1970)
53. Zel'dovich Ya B et al. *J. Fluid Mech.* **144** 1 (1984)
54. Zel'dovich Ya B, Ruzmaikin A A *Sov. Phys. JETP* **51** 493 (1980); *Zh. Eksp. Teor. Fiz.* **78** 980 (1980)
55. Zeldovich Ya B, Ruzmaikin A A *Sov. Sci. Rev. E* **2** 333 (1983)
56. Ivanova T S, Ruzmaikin A A *Sov. Astron.* **20** 227 (1976); *Astron. Zh.* **53** 398 (1976)
57. Ivanova T S, Ruzmaikin A A *Sov. Astron.* **21** 479 (1977); *Astron. Zh.* **54** 846 (1977)
58. Ivanova T S, Ruzmaikin A A *Sov. Astron.* **24** 75 (1980); *Astron. Zh.* **57** 127 (1980)
59. Roberts P H, Stix M *Astron. Astrophys.* **18** 453 (1972)
60. Soward A M *Astron. Nachr.* **299** 25 (1978)
61. Soward A M *Geophys. Astrophys. Fluid Dyn.* **64** 163 (1992)
62. Soward A M *Geophys. Astrophys. Fluid Dyn.* **64** 201 (1992)
63. Vainshtein S I, Zel'dovich Ya B, Ruzmaikin A A *Turbulentnoe Dinamo v Astrofizike* (Turbulent Dynamo in Astrophysics) (Moscow: Nauka, 1980)
64. Petrovay K *Astron. Nachr.* **328** 789 (2007)
65. Kitchatinov L L *Astron. Rep.* **45** 816 (2001); *Astron. Zh.* **78** 934 (2001)
66. Kitchatinov L L, Olemskoy S V *Astron. Lett.* **37** 656 (2011); *Pis'ma Astron. Zh.* **37** 713 (2011)
67. Belvedere G, Kuzanyan K M, Sokoloff D D *Mon. Not. R. Astron. Soc.* **315** 778 (2000)
68. Brandenburg A, Subramanian K *Phys. Rep.* **417** 1 (2005)
69. Choudhuri A R *Astron. Astrophys.* **253** 277 (1992)
70. Choudhuri A R, Shussler M, Dikpati M *Astron. Astrophys.* **303** 29 (1995)
71. Dikpati M, Charbonneau P *Astrophys. J.* **518** 508 (1999)
72. Dikpati M, Gilman P A *Astrophys. J.* **559** 428 (2001)
73. Kitchatinov L L, Olemskoy S V *Astron. Nachr.* **332** 496 (2011)
74. Kitchatinov L L, Rudiger G, Kuker M *Astron. Astrophys.* **292** 125 (1994)
75. Kitchatinov L L, Olemskoy S V *Solar Phys.* **276** 3 (2012)
76. Pipin V V, Sokolov D D, Usoskin I G *Astron. Astrophys.* **542** 26 (2012)
77. Pipin V V, Kosovichev A G *Astrophys. J.* **738** 104 (2011)
78. Pipin V V, Kosovichev A G *Astrophys. J.* **776** 36 (2013)
79. Baliunas S L et al. *Astrophys. J.* **460** 848 (1996)
80. Belvedere G, Paterno L, Stix M *Astron. Astrophys.* **91** 328 (1980)
81. Kitchatinov L L *Astron. Lett.* **28** 626 (2002); *Pis'ma Astron. Zh.* **28** 695 (2002)
82. Kuzanyan K M, Sokoloff D D *Geophys. Astrophys. Fluid Dyn.* **81** 113 (1995)
83. Landau L D, Lifshitz E M *Quantum Mechanics*: *Non-Relativistic Theory* (Oxford: Pergamon Press, 1977); Translated from Russian: *Kvantovaya Mekhanika*: *Nerelyativistskaya Teoriya* (Moscow: Nauka, 1989)
84. Maslov V P, Fedoriuk M V *Semi-Classical Approximation in Quantum Mechanics* (Dordrecht: D. Reidel Publ. Co., 1981); Translated from Russian: *Kvaziklassicheskoe Priblizhenie dlya Uravnenii Kvantovoi Mekhaniki* (Moscow: Nauka, 1976)
85. Arnol'd V I et al. *Sov. Phys. JETP* **54** 1083 (1981); *Zh. Eksp. Teor. Fiz.* **81** 2052 (1981)
86. Ruzmaikin A et al. *Geophys. Astrophys. Fluid Dyn.* **52** 125 (1990)
87. Sokoloff D, Shukurov A, Ruzmaikin A *Geophys. Astrophys. Fluid Dyn.* **25** 293 (1983)
88. Isakov R et al. *Astrophys. Space Sci.* **80** 145 (1981)
89. Kuzanyan K M, Sokoloff D D *Astron. Astrophys.* **18** 129 (1999)
90. Galitski V M, Sokoloff D D *Geophys. Astrophys. Fluid Dyn.* **91** 147 (1999)
91. Sokoloff D, Fioc M, Nesme-Ribes E *Magnetohydrodynamics* **31** 18 (1995); *Magn. Gidrodin.* **31** 19 (1995)
92. Galitski V M, Sokoloff D D, Kuzanyan K M *Astron. Rep.* **49** 337 (2005); *Astron. Zh.* **82** 378 (2005)
93. Makarov V I, Sivaraman K R *Solar Phys.* **85** 215 (1983)
94. Popova E P, Reshetnyak M Yu, Sokoloff D D *Astron. Rep.* **52** 157 (2008); *Astron. Zh.* **85** 183 (2008)
95. Popova H, Sokoloff D *Astron. Nachr.* **329** 766 (2008)
96. Popova E P *Astron. Rep.* **53** 863 (2009); *Astron. Zh.* **86** 928 (2009)
97. Kontor N N, Khotilovskaya T G *Sov. Astron.* **32** 211 (1988); *Astron. Zh.* **65** 414 (1988)
98. Ribes J C, Nesme-Ribes E *Astron. Astrophys.* **276** 549 (1993)
99. Sokoloff D D, Nesme-Ribes E *Astron. Astrophys.* **288** 293 (1994)
100. Benevolenskaya E E, Kosovichev A A, Schereer P H *Astrophys. J. Lett.* **554** 107 (2001)

101. Harvey K L, in *The Solar Cycle, Proc. of the National Solar Observatory, Sacramento Peak, 12th Summer Workshop* (ASP Conference Ser., Vol. 27, Ed. K L Harvey) (San Francisco, CA: ASP, 1992) p. 335
102. Meunier N et al. *Geophys. Astrophys. Fluid Dyn.* **86** 249 (1997)
103. Kuzanyan K M, Sokoloff D D *Astron. Rep.* **40** 424 (1996); *Astron. Zh.* **73** 469 (1996)
104. Bassom A P, Kuzanyan K M, Soward A M *Proc. R. Soc. Lond. A* **455** 1443 (1999)
105. Belvedere G, Kuzanyan K M, Sokoloff D D *Mon. Not. R. Astron. Soc.* **315** 778 (2000)
106. Huerre P, Monkewitz P A *Annu. Rev. Fluid Mech.* **22** 473 (1990)
107. Soward A M, Jones C A *Mech. Appl. Math.* **36** 19 (1983)
108. Starchenko S V, Kono M *Geophys. Astrophys. Fluid Dyn.* **82** 93 (1996)
109. Belvedere G M, Proctor M R E, Lanzafame G *Nature* **350** 481 (1991)
110. Ruzmaikin A A, Starchenko S V *Sov. Astron.* **31** 552 (1987); *Astron. Zh.*. **64** 1057 (1987)
111. Ruzmaikin A A, Sokoloff D D, Starchenko S V *Solar Phys.* **115** 5 (1988)
112. Makarov V I, Ruzmaikin A A, Starchenko S V *Solar Phys.* **111** 267 (1987)
113. Hathaway D H *Living Rev. Solar Phys.* **7** 1 (2010)
114. Komm R W, Howard R F, Harwey J W *Solar Phys.* **147** 207 (1993)
115. Zhao J, Kosovichev A *Astrophys. J.* **603** 776 (2004)
116. Brajsa R, Wouhl H *Hvar Observatory Bull.* **24** 125 (2001)
117. Lustig L, Wouhl H *Astron. Astrophys.* **249** 528 (1991)
118. Tuominen J, Tuominen I, Kyrolainen J *Mon. Not. R. Astron. Soc.* **205** 691 (1983)
119. Tuominen J *Z. Astrophys.* **51** 91 (1961)
120. Tuominen J, Kyrolainen J *Solar Phys.* **79** 161 (1982)
121. Tuominen J *Astrophys. J.* **143** 266 (1966)
122. Tuominen J *Solar Phys.* **34** 15 (1973)
123. Tuominen J *Z. Astrophys.* **37** 145 (1955)
124. Olemskoy S V, Kitchatinov L L *Astron. Lett.* **31** 706 (2005); *Pis'ma Astron. Zh.* **31** 793 (2005)
125. Olemskoi S V, Kichatinov L L *Izv. Ross. Akad. Nauk Ser. Fiz.* **70** 1427 (2006)
126. Ivanov E V, Obridko V N, Shelting B D, in *Solar Variability as an Input to the Earth's Environment: Intern. Solar Cycle Studies, ISCS Symp., 23–28 June 2003, Tatranská Lomnica, Slovak Republic* (ESA, SP-535, Ed. A Wilson) (Noordwijk: ESA Publ., 2003) p. 37
127. Bonanno A et al. *Astron. Astrophys.* **390** 673 (2002)
128. Obridko V N, Shelting B D *Astron. Rep.* **47** 953 (2003); *Astron. Zh.* **80** 364 (2003)
129. Durrant C J, Turner J P R, Wilson P R *Solar Phys.* **222** 345 (2004)
130. Ivanov E V, Obridko V N *Solar Phys.* **206** 1 (2002)
131. Kitchatinov L L *Astron. Rep.* **48** 153 (2004); *Astron. Zh.* **81** 176 (2004)
132. Kitchatinov L L, Rudiger G *Astron. Nachr.* **325** 496 (2004)
133. Soward A M et al. *Geophys. Astrophys. Fluid Dyn.* **107** 667 (2013)
134. Popova E P *Astron. Lett.* **37** 210 (2011); *Pis'ma Astron. Zh.* **37** 233 (2011)
135. Starchenko S V *Astron. Rep.* **39** 227 (1995); *Astron. Zh.* **72** 257 (1995)
136. Bassom A P et al. *Geophys. Astrophys. Fluid Dyn.* **99** 309 (2005)
137. Griffiths G L et al. *Geophys. Astrophys. Fluid Dyn.* **94** 85 (2001)
138. Meunier N, Nesme-Ribes E, Sokoloff D D *Astron. Rep.* **40** 415 (1996); *Astron. Zh.* **73** 460 (1996)
139. Ponty Y, Bassom A P, Soward A M, in *Dynamo and Dynamics, a Mathematical Challenge* (NATO Science Ser. II, Vol. 26, Eds P Chossat, D Armbruster, I Oprea) (Boston: Kluwer Acad. Publ., 2001)
140. Starchenko S V *Geophys. Astrophys. Fluid Dyn.* **77** 55 (1994)
141. Ruzmaikin A A *Comments Mod. Phys. C* **9** 85 (1981)
142. Kitiashvili I, Kosovichev A G *Astrophys. J.* **688** 49 (2008)
143. Kitiashvili I, Kosovichev A G *Geophys. Astrophys. Fluid Dyn.* **103** 53 (2009)
144. Sokoloff D D, Nefedov S N *Vychisl. Metody Programmirovanie* **8** 195 (2007)
145. Nefedov S N, Sokoloff D D *Astron. Rep.* **54** 247 (2010); *Astron. Zh.* **87** 278 (2010)
146. Sokoloff D D et al. *Astron. Lett.* **34** 761 (2008); *Pis'ma Astron. Zh.* **34** 842 (2008)
147. Arlt R *Solar Phys.* **255** 143 (2009)
148. Illarionov E et al. *Astron. Nachr.* **332** 590 (2011)
149. Moss D, Saar S H, Sokoloff D *Mon. Not. R. Astron. Soc.* **388** 416 (2008)
150. Popova E P *Astron. Rep.* **57** 310 (2013); *Astron. Zh.* **90** 347 (2013)
151. Popova H *Magnetohydrodynamics* **49** 59 (2013)
152. Popova E P, Yukhina N A *Astron. Lett.* **39** 729 (2013); *Pis'ma Astron. Zh.* **39** 810 (2013)
153. Popova E P, Potemina K A *Geomagn. Aeron.* **53** 941 (2013)
154. Popova E P, Potemina K A, Yukhina N A *Geomagn. Aeron.* **54** 877 (2014)
155. Obridko V N, Shelting B D *Adv. Space Res.* **40** 1006 (2007)
156. Benevolenskaya E *Solar Phys.* **161** 1 (1995)
157. Benevolenskaya E *Solar Phys.* **216** 325 (2003)
158. Krivova N A, Solanki S K *Astron. Astrophys.* **394** 701 (2002)
159. Richardson J D et al. *Geophys. Res. Lett.* **21** 1559 (1994)
160. Mursula K, Zieger B *Adv. Space Res.* **25** 1939 (2000)
161. Mursula K et al. *Solar Phys.* **221** 201 (2003)
162. Obridko V N et al. *Mon. Not. R. Astron. Soc.* **365** 827 (2006)
163. Obridko V N, Shelting B D *Astron. Rep.* **45** 1012 (2001); *Astron. Zh.* **78** 1146 (2001)
164. Apostolov E V *Bull. Astron. Inst. Czech.* **36** 97 (1985)
165. Benevolenskaya E E *Solar Phys.* **191** 247 (2000)
166. Parker E N *Astrophys. J.* **163** 252 (1971)
167. Vainshtein S I, Ruzmaikin A A *Sov. Astron.* **15** 714 (1972); *Astron. Zh.* **48** 902 (1971)
168. Vainshtein S I, Ruzmaikin A A *Sov. Astron.* **16** 365 (1972); *Astron. Zh.* **49** 449 (1972)
169. Widrow L M *Rev. Mod. Phys.* **74** 775 (2002)
170. Priklonsky V et al. *Geophys. Astrophys. Fluid Dyn.* **93** 97 (2000)
171. Willis A P et al. *Geophys. Astrophys. Fluid Dyn.* **98** 345 (2004)
172. Baryshnikova Yu et al. *Astron. Astrophys.* **177** 27 (1987)
173. Stepinski T F, Levy E H *Astrophys. J.* **379** 343 (1991)
174. Krasheninnikova Yu et al. *Astron. Astrophys.* **213** 19 (1989)
175. Starchenko S V, Shukurov A *Astron. Astrophys.* **214** 47 (1989)
176. Kvasz L, Sokoloff D D, Shukurov A M *Geophys. Astrophys. Fluid Dyn.* **65** 231 (1992)
177. Poezd A, Shukurov A M, Sokoloff D D *Mon. Not. R. Astron. Soc.* **264** 285 (1993)
178. Cattaneo F, Hughes D W, Kim E *Phys. Rev. Lett.* **76** 2057 (1996)
179. Stepinski T F, Levy E H *Astrophys. J.* **331** 416 (1988)
180. Elstner D, Meinel R, Rudiger G *Geophys. Astrophys. Fluid Dyn.* **50** 85 (1990)
181. Sokoloff D, Shukurov A *Nature* **347** 51 (1990)
182. Brandenburg A et al. *Astron. Astrophys.* **259** 453 (1992)
183. Brandenburg A et al. *Astron. Astrophys.* **271** 26 (1993)
184. Brandenburg A, Moss D, Shukurov A *Mon. Not. R. Astron. Soc.* **276** 651 (1995)
185. Elstner D et al. *Astron. Astrophys.* **297** 77 (1995)
186. Moss D, Shukurov A, Sokoloff D *Astron. Astrophys.* **343** 120 (1999)
187. Moss D, Shukurov A, Sokoloff D *Astron. Astrophys.* **358** 1142 (2000)
188. Moss D, Shukurov A *Astron. Astrophys.* **372** 1048 (2001)
189. Moss D, Shukurov A *Astron. Astrophys.* **413** 403 (2004)
190. Mestel L, Subramanian K *Mon. Not. R. Astron. Soc.* **265** 649 (1993)
191. Moss D *Mon. Not. R. Astron. Soc.* **275** 191 (1995)
192. Phillips A *Geophys. Astrophys. Fluid Dyn.* **94** 135 (2001)
193. Chamandy L, Subramanian K, Shukurov A *Mon. Not. R. Astron. Soc.* **433** 3274 (2013)
194. Chamandy L, Subramanian K, Shukurov A *Mon. Not. R. Astron. Soc.* **428** 3569 (2013)